

9. CELL GROWTH AND DIVISION

13 January 2023

The central mission of all cells – to survive and reproduce – is a product of the relentless operation of natural selection. For unicellular organisms, the matter of cellular reproduction naturally brings us into contact with the issue of cellular growth. Typically, cells double in size and then reproduce by binary fission, although there are cases in which offspring and adult cell sizes differ by more than two-fold, e.g., budding in some yeast, and multiple internal fissions in some algae. The essential issue is that continuous proliferation of a population requires the growth and division of individual cells, which requires the intake and conversion of nutrients to biomolecules.

Here, we focus on several general challenges that exist for any growth mechanism, deferring the molecular details on resource uptake and cell fission to subsequent chapters (10 and 18, respectively). First, cell growth requires coordination between the intake of resources and their conversion into cellular material. Even the simplest of cells consist of thousands of types of molecules, so the overall process may seem hopelessly beyond mechanistic interpretation. However, some aspects of cell growth can be understood in general terms using models incorporating a minimum level of molecular complexity.

Second, in relating growth in cellular biomass to the matter of reproduction, the issue arises as to how a cell decides when to undergo fission. In principle, cells might simply divide after a critical time period has passed, although this would require slowing the clock down in nutrient-poor environments. Alternatively, division might be delayed until a critical cell size (possibly environmentally determined) is reached. Still another possibility is that the license to divide is based on the attainment of a specific growth increment, in which case the size at division would be defined by the prior size at birth. Regardless of the target criterion, cells must generally possess compensatory mechanisms to prevent runaway growth or diminution in size in extreme individuals.

Third, cell division is not a perfect process. Some size variation among sister cells always results from binary fission, and this is inevitably accompanied by variance in the partitioning of the parental-cell contents. Entirely a consequence of the limits to the perfection of cell-division mechanisms, such variation generates phenotypic variation even in otherwise genetically uniform populations, and at a level that is potentially much higher than in multicellular species. Some have argued that the production of phenotypic variation has been promoted by natural selection as a bet-hedging strategy to cope with heterogeneous environments. However, as discussed below, nongenetic sources of phenotypic variation reduce the efficiency of natural selection and impose long-term fitness loads, leaving many open questions on this matter.

The following pages attempt to summarize what we know about these issues. Remarkably, however, the depth of understanding of the mechanistic determinants of the emergent properties of size and growth rate lags that for many of the more intricate and lower-level molecular features of cells.

Ribosomes and Cell Growth

Given that protein constitutes a large fraction of cell mass, before considering the more quantitative aspects of growth, an overview of the molecular machine dedicated to protein production is in order. Cells make enormous investments in ribosomes, with up to 50% of all transcription being devoted to the production of ribosomal RNA (rRNA, the catalytic heart of the ribosome) and up to 50% of messenger RNA (mRNA) production allocated to the production of ribosomal proteins (Warner et al. 2001). Each ribosome can process only one mRNA at a time, and ribosomes are energetically expensive to produce, so strong regulatory associations between cellular growth rates and the number of ribosomes per cell can be expected. Overly low numbers of ribosomes relative to the cellular supply of nutrients compromises the rate of production of cellular biomass, but excess investment in ribosomes diverts energy from other cellular processes essential to resource acquisition.

Consistent with this expectation, for all species in which the issue has been addressed, there is a strong and essentially linear relationship between cell growth rate and the ratio of total RNA to total protein mass in the cell (Figure 9.1A). In other words, there is a predictable shift in the molecular contents of cells as they are exposed to more nutrient-rich environments. Generally, the RNA/protein mass ratio is in the range of 0.1 to 0.2 at low growth rates, and then increases to ~ 0.5 or even more in the fastest growing cells. These types of responses are retained even when the growth-rate differences are created by varying the types of substrates (as opposed to altering the concentration of a single limiting nutrient) (Schaechter et al. 1958; Fraenkel and Neidhardt 1961). Thus, the level of RNA production is regulated by an indirect connection with the growth rate itself, rather than by direct resource-specific signals.

Although the patterns illustrated in Figure 9.1A refer to the total RNA in a cell, additional data suggest a coordinated response for mRNAs, tRNAs, and rRNAs, such that the number of ribosomes per cell also scales directly with the cellular growth rate. For most species that have been examined, the ratio of rRNA to total RNA in cells falls in the range of 0.55 to 0.88, typically not deviating by more than 0.15 between different growth rates (Figure 9.1B). Thus, with increasing nutrient availability, the number of ribosomes per cell increases in a coordinated way with the growth rate.

Such proportionality arises from various feedback mechanisms. Ribosome biogenesis is often controlled indirectly by the level of free rRNA in the cell, the production of which is in turn regulated via the amount of uncharged tRNAs (Liu et al. 2015). In *E. coli*, for example, an alarmone (guanosine tetraphosphate or ppGpp) is produced when uncharged tRNAs (transfer RNAs unattached to amino acids) accumulate in the face of an inadequate supply of amino acids, and the reduced translational rate of elongation suppresses rRNA production (Potrykus et al.

2011; Wu et al. 2022). When ribosomal proteins are in excess in the cell relative to the rRNAs with which they must assemble, the former bind to their own mRNAs, thereby repressing their own production. In contrast, in the soil bacterium *Bacillus subtilis*, inhibition of rRNA production results from a drop in cellular GTP levels (a result of enhanced incorporation of GTP into ppGpp) (Krásný and Gourse 2004). A variety of other mechanisms exist in eukaryotes (Warner et al. 2001; Parenteau et al. 2019). Such evolutionary wandering of mechanisms regulating otherwise highly conserved functions will be encountered for a number of other cellular traits in the following pages.

A relatively simple theoretical argument potentially explains the linear relationship between investment in ribosomes and growth rate (Foundations 9.1). Assuming that all but a small fixed fraction of ribosomes is actively engaged in translation and that active ribosomes are generally saturated with mRNAs, the overall growth rate can only be enhanced by increasing the translation rate per ribosome and/or the number of ribosomes per cell. For species with available data, translation rates per ribosome generally change by no more than a factor of two over a scale in which the cell growth rate varies by up to two orders of magnitude (Figure 9.1C). Thus, elevated investment in ribosomes appears to be the dominant mechanism by which cells increase protein production.

Under this view, a plot of the mass ratio of ribosomal protein to total protein against the cell growth rate (Equation 9.1.3) has a specific biological meaning – the y intercept is a measure of the investment in inactive ribosomes relative to the total pool of proteins, and the inverse of the slope is a measure of the rate of protein mass produced per mass of ribosomal protein. Figure 9.1A provides such a plot for *E. coli*, except that the y -axis values need to be multiplied by 0.53 to convert to the ribosomal protein ratio for this species (Scott et al. 2010). Although *E. coli* will be used as an exemplar in the following analyses, this species has a distinctly lower intercept and slope for the response plot than in other species, meaning that *E. coli* achieves a maximum growth rate with a relatively low investment in RNA (and presumably ribosomes).

The total investment in ribosomal proteins in *E. coli* can be obtained by multiplying the total RNA/total protein mass ratio by the average rRNA/total RNA ratio of 0.62 from Dennis and Bremer (1974), and then by the ratio of ribosomal protein to rRNA mass of 0.53. From Figure 9.1A, this leads to the conclusion that $\sim 3\%$ of the protein in a nongrowing *E. coli* cell is associated with ribosomes. This is in reasonable agreement with a more direct estimate of $\sim 8\%$ associated with nontranslating ribosomes in budding yeast (Metzl-Raz et al. 2017). Although little work has been done on the matter, in *E. coli*, and likely other bacteria, ribosomes dimerize and become translationally quiescent under nutritionally starved states (Vila-Sanjurjo 2008; Yoshida and Wada 2014). A non-zero reserve at near-zero growth rate is not too surprising, as complete ribosome loss sentences a cell to death by eliminating any possibility of responding to improved nutrient conditions (Mori et al. 2017).

The fractional investment in ribosomal proteins increases to 28% for cells growing at maximum rate, and when the total amount of accessory proteins associated with translation is added in, this number needs to be multiplied by ~ 1.7 to determine the total investment in the process of translation (Scott et al. 2010). Thus, a rapidly growing *E. coli* cell devotes nearly 50% of its protein to translation. Al-

though the data are less extensive, eukaryotes have higher total RNA/total protein and rRNA/total RNA mass ratios than bacteria (Figure 9.1A,B), as well as higher numbers of ribosomal proteins per ribosome (Chapter 6). This means that to achieve equivalent growth rates eukaryotic cells must make an even larger fractional investment in ribosome production than prokaryotes.

The results in Figure 9.1 can also be used to estimate the absolute upper bound on the growth rate, by considering the expected division time of a hypothetical cell consisting of nothing but translational machinery. The inverse of the slope in Figure 9.1A implies a rate of protein mass produced per unit ribosome mass per hour of 7.5. In other words, a healthy *E. coli* ribosome can replace its own protein constituents in about $60/7.5 = 8$ minutes.

The upper limit to the growth rate can also be calculated more directly by considering the number of amino acids per ribosome and the upper bound to the rate of translation (again, assuming that the cell consists of nothing but actively engaged translation machinery). The full set of bacterial ribosomal proteins comprising an individual ribosome contains $\sim 7,500$ amino acids, and the upper bound to the translation rate is ~ 20 amino acids/ribosome/second (Figure 9.1C). If one then liberally assumes that an extended ribosome (the complete translational machinery) contains twice as many amino acids as the ribosome itself, then the time required for complete replacement of an extended ribosome rate is $(2 \cdot 7500)/20 = 750$ seconds, or 12.5 minutes, in excellent agreement with the prior calculation (which ignored accessory proteins).

Thus, without an increase in the rate of translation or a decrease in the size of an extended ribosome, the cell-division time in an *E. coli*-like bacterium cannot be reduced below ~ 12.5 minutes, indicating that the massive cost of the ribosome itself imposes a significant limit on the rate of cell division. Under optimal growth conditions, some bacteria such as *Vibrio natriegens* have doubling times very close to this ultimate limit (Chapter 8).

Models for Cellular Growth

Natural selection promotes phenotypes that maximize the rate of entry of progeny into the subsequent generation, which requires both reproduction and survival. Here, we consider the issues in a very general sense, with an initial focus on simple expressions for the response of cell-division rates to the concentration of a limiting nutrient, e.g., glucose for a laboratory-grown bacterium, or phosphorus for a planktonic alga. This will then be followed by an exploration of how cell size and division time are set and interrelated.

As discussed below, even in a constant environment, substantial variation typically exists in the division times of individual cells, owing to internal stochastic processes. Nonetheless, an ensemble of cells can be described by the average population-level rate of increase r . Letting N_0 and N_t denote population sizes at two points in time, then assuming constant conditions,

$$N_t = N_0 e^{rt} \tag{9.1}$$

describes the trajectory of numbers of individuals over this period (Foundations

9.1). Defined in this way, r is a measure of the per-capita exponential growth rate (with units of time^{-1}). Taking logarithms and rearranging,

$$r = \frac{\ln N_t - \ln N_0}{t}. \quad (9.2)$$

The doubling time for population size, obtained by setting $N_t/N_0 = 2$, is

$$t_d = \ln(2)/r. \quad (9.3)$$

Like interest in a bank account, the doubling time of $\simeq 0.693/r$ is less than expected under linear growth.

The preceding expressions apply to the special situation in which a population is expanding in a nutritionally constant environment, but of course, no population can grow exponentially for an indefinite period of time. In more general applications in population biology, r is usually used to describe the actual rate of population growth, which reflects the net difference between birth and death rates, $r = b - d$. In this chapter, however, the focus is primarily on laboratory cultures, where there is typically very little direct cell death. In that case, r can be viewed as the rate of cell birth ($r \simeq b$ because $d \simeq 0$), which with a constant steady-state distribution of cell sizes at division, is equivalent to the exponential rate of increase in cellular biomass (Jun et al. 2018). In a laboratory culture where cells are being regularly drawn off (as in a chemostat; Figure 8.3), the birth rate can be kept indefinitely at a constant level (equal to the dilution rate, d , because $r = b - d = 0$ within the growth chamber).

From observations on bacteria grown under constant conditions, Monod (1949) concluded that the growth-rate response to a limiting nutrient concentration (S) can be described by a simple hyperbolic function,

$$r = r_{\max} \left(\frac{S}{K_r + S} \right), \quad (9.4a)$$

where r_{\max} is the maximum rate of growth (asymptotically approached as $S \rightarrow \infty$), and K_r is the half-saturation constant for growth (equivalent to the resource concentration at which $r = r_{\max}/2$). As will be discussed in Chapter 18, this formula is identical in form to the commonly employed Michaelis-Menten equation for nutrient uptake and other enzymatic reactions,

$$u = u_{\max} \left(\frac{S}{K_u + S} \right), \quad (9.4b)$$

where K_u is the half-saturation constant for uptake, which is not necessarily equal to K_r .

Numerous other models have been proposed to link growth rate to nutrient availability. For example, with a focus on algal cells in continuous culture, Droop (1973, 1974) considered a construct in which the growth rate depends on the *internal* cellular concentration of the limiting nutrient (Q , commonly referred to as the cell quota),

$$r = r_{\max} \left(1 - \frac{\phi}{Q} \right). \quad (9.5)$$

Under this model, cell division ceases when Q drops below the critical internal concentration ϕ , and r asymptotically approaches the maximum possible value r_{\max} as the internal nutritional state Q increases. An attractive feature of this expression is that cell growth is more naturally connected with internal than external nutrient levels. Although internal nutrient pools are not necessarily easy to estimate, measures of r and Q in nutrient-limited cultures of single species of phytoplankton have repeatedly supported the general form of Equation 9.5 (Figure 9.2).

Despite its different functional underpinnings, the structure of Equation 9.5 is entirely compatible with the Monod growth equation. This can be seen by noting that for a system in steady-state, the rate of nutrient uptake must equal the product of the cell quota and the rate of cell growth, i.e., $u = r \cdot Q$, which implies a cell quota equal to the ratio of rates of uptake and growth, $Q = u/r$. Substituting this expression into Equation 9.5 and rearranging yields

$$r = r_{\max} \left(\frac{u}{(r_{\max}\phi) + u} \right), \quad (9.6)$$

which again has the form of a hyperbolic relationship, in this case between r and the rate of nutrient uptake. If Equation 9.4b is substituted for u here, a more complex expression is obtained in terms of S and the uptake parameters, but this is still hyperbolic with respect to the external nutrient concentration S , recovering the form of Equation 9.4a.

Equations 9.4a and 9.5 have been used to describe thousands of growth responses, and are often referred to as growth laws. However, the models are phenomenological in the sense that they do not explicitly describe any of the underlying cellular mechanisms connecting substrate uptake, utilization, and growth. They simply describe general growth responses to nutrient limitation with a minimum amount of detail. More complex models have been proposed. For example, Maitra and Dill (2015) and Weiße et al. (2015) presented formulations that include ribosomes, other RNAs, protein, and ATP as the underlying variables, in both cases generating predictions that are consistent with the Monod-growth model and ribosome-growth coupling noted above. Models with an intermediate level of complexity, describing r_{\max} and K_r in mechanistic terms associated with the translational capacity of ribosomes and the nutritional capacity of the environment are outlined in Foundations 9.2. These provide a satisfying explanation for the response of ribosome investment to increased nutrient availability noted in the preceding section.

Control of Cell Size

As discussed in the previous chapter, cell volumes vary by approximately eleven orders of magnitude among unicellular species. Within-species variation also exists as a consequence of prevailing environmental conditions, stochastic variation in cell volume arising during division, and position in the cell-division cycle (age variation). Nonetheless, under any particular environmental setting, the range of cell sizes within a species is generally fairly narrow, with standard deviations well below the mean. This implies the existence of homeostatic mechanisms for cell-size regulation.

Under constant conditions, the average rate of increase in cell size (per unit biomass) between divisions must equal the average rate of increase in cell number, i.e., the rate of cell division. If this were not the case, cell size would become progressively smaller or larger. In other words, at steady state, cells must double in size at the same rate that the population doubles in cell number. This, however, leaves open the possibility of a diversity of patterns of biomass growth within the life span of a cell. Resolving this issue is critical to understanding how cell size and division time are jointly determined.

As outlined above, the numbers of cells within expanding populations kept at constant environmental conditions increase exponentially in time. If individual cells grew in a parallel manner, under steady-state conditions, cell volume would grow in accordance with Equation 9.1,

$$V_t = V_0 e^{rt}, \quad (9.7)$$

where V_0 is the size of a newborn cell, and V_t is its size t time units later. Under this model, the proportional rate of change in cell volume is independent of cell size, although larger cells grow more rapidly in an absolute sense.

Exponential growth specifically implies that the metabolic features of growing cells remain constant, independent of size, with the ensemble of constituent molecules operating via a fixed set of reaction rates per unit cytoplasmic volume. However, exponential growth in cell size is not essential for balanced growth. The only requirement is that cumulative cellular biomass doubles from birth to death, i.e., matches the rate of increase in cell number. In principle, growth might be linear, with the rate of acquisition of biomass being independent of cell size, or sigmoidal, with the rate of cell growth initially accelerating and then decelerating as a critical size is approached.

Nonetheless, observations on the growth of individual cells for multiple bacterial species support the exponential cell-growth model (or something very close to it) (Voorn and Koppes 1998; Santi et al. 2013; Iyer-Biswas et al. 2014; Osella et al. 2014; Campos et al. 2014; Susman et al. 2018), with no known striking exceptions. In addition, this particular model extends to eukaryotes. Godin et al. (2010) and Bryan et al. (2010) observed exponential growth not only in the bacteria *E. coli* and *B. subtilis*, but also in the yeast *S. cerevisiae* and mouse lymphoblast cells, and similar observations have been made on human osteosarcoma cells (Mir et al. 2011) and in the ciliate *Paramecium tetraurelia* (Kimball et al. 1959).

In terms of cell-size homeostasis, however, there remains a problem. Owing to stochasticities arising during division, not all cells have exactly the same size at birth. How then are the sizes of consecutive cells produced within a lineage regulated so as to prevent overly small/large cells from spawning ever more extreme descendants? If cells simply grew exponentially for a specified time before division, following a timer model, those that were larger at birth would grow more over the specified duration, leading to a potentially runaway size distribution (Figure 9.3). Under an alternative sizer model, cells might be programmed to divide once a critical volume is reached.

For the best-studied organism, *E. coli*, both of these models come up short. Instead, for a given environment, cells appear to add an approximately constant volume (Δ) prior to division (Taheri-Araghi et al. 2015) (Figure 9.4). This adder model leads to a simple mechanism of cell-size homeostasis, with the steady-state

expected offspring size being equal to Δ . Contrary to the sizer model, the adder model predicts that larger newborn cells will divide at larger sizes (with expected volume $V_0 + \Delta$), in effect being oblivious to their initial size. Nonetheless, with Δ remaining independent of size, the adder model also predicts that cells with extreme size will produce descendants progressively returning to the expected size Δ . The simple basis for such homeostasis can be seen by the following argument.

If a newborn cell is larger than Δ , say by an amount v , then cell division will occur at expected size $(v + \Delta) + \Delta = v + 2\Delta$, and the average offspring size will be half that, $(v/2) + \Delta$, and hence shifted back towards the long-term expected value Δ by an amount $v/2$. The opposite (a shift towards larger offspring size) occurs if an offspring cell happens to be slightly smaller than Δ . In both cases, the deviations from the expected newborn size decline over time, insuring rapid convergence back to Δ . These arguments ignore new deviations that arise at each subsequent division, and the actual damping process is less smooth than this simple description implies (Tanouchi et al. 2015), with individual cells having unique response behaviors, presumably reflecting idiosyncratic stochasticities (Susman et al. 2018). Nonetheless, the overall condition of homeostasis is retained.

As can be seen in Figure 9.4, the behavior of *E. coli* cells at the extreme ends of the size spectrum deviates slightly from the expectations of this simple adder model, which assumes independence between the parental cell size and the subsequent growth increment. Instead, the latter appears to decline with increasing cell size. Such second-order effects can be accommodated by a simple modification of the growth-increment expression (Delarue et al. 2017; Jun et al. 2018; Susman et al. 2018). Consider, for example, the situation in which there is some memory of parental cell-size at birth (V_p) such that the predicted offspring size is $V_0 = \alpha V_p + \Delta$. Setting $V_0 = V_p$ yields an equilibrium cell size of $\Delta/(1-\alpha)$, which implies homeostasis provided $-1 < \alpha < 1$. If $\alpha < -1$, cell-size declines to zero, whereas $\alpha > 1$ leads to runaway cell growth.

This more general model accommodates a wide range of species. The one member of the archaea in which the growth properties have been investigated, *Halobacterium salinarum*, appears to adhere closely to the pure adder model (Eun et al. 2017). However, two bacterial species with asymmetric cell division, *Caulobacter crescentus* (Campos et al. 2014; Iyer-Biswas et al. 2014) and *Mycobacterium smegmatis* (Santi et al. 2013; Logsdon et al. 2017; Priestman et al. 2017), as well as the symmetrically dividing bacterium *Pseudomonas aeruginosa* (Deforet et al. 2015) have slightly positive values of $0 < \alpha < 1$. In contrast, budding yeast *S. cerevisiae* (Di Talia et al. 2007; Soifer and Barkai 2014; Soifer et al. 2016; Chandler-Brown et al. 2017) and fission yeast *S. pombe* (Fantès 1977; Svecizer et al. 1996) have negative values of α .

Finally, the form of a growth model has implications for response of cell-division time to size at birth. For example, under an adder model of cell division, cells that are larger at birth divide at an earlier age because the additive increment Δ is achieved more rapidly. From the form of the exponential-growth model (Equation 9.7), the division time for a cell of initial size V_0 under the pure adder model is

$$t_d = \frac{\ln[1 + (\Delta/V_0)]}{r}, \quad (9.8)$$

yielding a predicted decline in t_d with increasing V_0 , consistent with observations

in *E. coli* (Figure 9.4). As discussed below, in a dynamically growing population, this may lead to an equilibrium mean offspring size $> \Delta$, as offspring of large-size deviants will be promoted into the population at a higher rate than those of small-size deviants.

Molecular mechanisms of division-size determination. The simple models just outlined provide a statistical view of the features of cell division, but leave unanswered questions as to the molecular mechanisms enabling cells to determine when they have reached the critical threshold for division. Resolving these issues is essential to understanding how changes in cell sizes and division times might be accomplished by evolution.

One model for this decision-making process invokes a burst of cell-division inhibitor produced at the time of cell division, which then gradually becomes diluted as cell volume increases. An alternative model invokes the gradual buildup of an activator molecule to the point at which a threshold concentration is exceeded. Simple mathematical constructs have been developed to explain the features of these alternative models (Sompayrac and Maaløe 1973; Amir 2014; Deforet et al. 2015; Soifer et al. 2016). However, for species in which the molecular underpinnings of cell-division time have been sought, inhibitor mechanisms have generally come to the fore (Figure 5).

For example, the soil bacterium *Bacillus subtilis* determines the time of cell division by use of a two-component system (Weart et al. 2007; Chien et al. 2012). The tubulin-like cell-division protein (FtsZ) acts as a central hub and has a nearly constant concentration under all nutritional conditions. At high nutrient conditions, an inhibitor molecule (UgtP) oligomerizes with FtsZ preventing formation of the cytokinetic ring until a relatively large cell size (diluting UgtP, and freeing up FtsZ molecules) is attained. Under low nutrient conditions, UgtP is sequestered away from FtsZ, allowing division at a smaller cell size.

E. coli utilizes a different inhibitor mechanism to determine the time of division. In this case, an inhibitor molecule oscillates back and forth between the cell poles, such that a minimum concentration exists at the cell midpoint. Once the inhibitor concentration drops below a critical point by growth dilution, cell division ensues (Lutkenhaus 2008).

Inhibitor mechanisms for division-time determination extend to yeasts. The fission yeast *S. pombe* utilizes a spatial gradient to sense its size – an activator of mitosis is centrally located, whereas an inhibitor of the activator has a gradient initiating at the cell poles; as the cell grows, the inhibitor concentration declines to the point at which mitosis is activated (Moseley et al. 2009). In contrast, in the budding yeast *S. cerevisiae*, a short burst of synthesis of a mitosis inhibitor is elicited shortly after cell division in a size-independent manner (Turner et al. 2012; Schmoller et al. 2015; Litsios et al. 2019). Smaller cells, with a higher inhibitor concentration at birth, must then add more volume to reduce the inhibitor to its critical concentration to allow mitosis to proceed. A second protein, plays a central role here, operating as an inhibitor of the mitotic inhibitor, but only becoming effective upon increasing in abundance late in the growth cycle and reducing the mitotic inhibitor to a low enough level to allow division initiation.

Remarkably, although all four of these systems rely on mechanisms of inhibition

to determine cell-division time, the molecular details are essentially nonoverlapping. As in the case of the regulation of ribosome biogenesis (Chapter 6), this implies that over evolutionary time the basic machinery dictating the key life-history features of cells – size and age of reproduction – has been rewired on multiple occasions. How such modifications are made without imperiling the fitness of individuals with intermediate states is unclear, and constitutes a major challenge for evolutionary cell biology. Regardless of the underlying evolutionary mechanisms, one should clearly be wary of Jacob’s (1998) proclamation that “All that is true for *E. coli*, is true for the elephant.”

The above models invoke the monitoring of some sort of molecule to indirectly forecast the appropriate time for division, but do so in a way that is notably agnostic with respect to genome replication processes. A related mechanistic proposal, not necessarily unconnected with the processes noted above, is that bacterial cell division is somehow guided by the state of genome replication (Wallden et al. 2016; Amir et al. 2017; Jun et al. 2018; Si et al. 2019), as is the case with the eukaryotic cell cycle (Chapter 10). The idea here is that bacteria growing at rapid rates experience pileups of partially replicated, nested genomes as the rate of genome replication lags behind the rate of production of the remaining cellular constituents. In one version of this model, the critical determining factor is the ratio between the number of genome origins of replication (the starting points of duplicating genomes) and cell volume (Jun et al. 2018; Si et al. 2019). This model fairly accurately fits the response of *E. coli* cell volume to cell growth rate, predicting an exponential response of cell size to growth rate, in accordance with some observations (below). The model also predicts that the negative scaling of cell-division time and size at birth will become increasingly strong in nutrient-poor environments, as has been seen (Figure 9.4).

However, there are two caveats with respect to this model. First, any number of other underlying division-time determinants beyond the numbers of origins of replication (but highly correlated with them) might play a key role. Indeed, rather different models, with a focus on partitioning of resources between ribosomes and unspecified division proteins, fit the data just as well (Bertaux et al. 2020; Serbanescu et al. 2020), and additional work suggests that DNA replication and cytoplasmic growth jointly influence the time to division (Colin et al. 2021). Second, an origin-counting model cannot apply to eukaryotes, which always undergo a single genome replication per cell division.

These rather unsettling uncertainties aside, the simple models outlined above (or variants of them) provide a clear path to understanding the molecular basis for evolutionary changes in cell size/division time via alterations in the concentrations and/or activities of the products of as few as two genes, e.g., an inhibitor molecule and its interacting partner. In principle, for example, larger cell size can be achieved by increasing the burst size of the mitotic inhibitor upon cell division or by reducing the sensitivity of its partner to inhibition.

Environmental determinants of cell size. Whatever the molecular mechanism of cell-size regulation, it is clear that the key parameters associated with the system must vary with environmental conditions. For example, cell size typically increases with nutrient availability, which under the adder model implies an increase in Δ . Such patterns have been clearly documented in *E. coli* (Taheri-Araghi et al. 2015;

Zheng et al. 2020), *Salmonella typhimurium* (Schaechter et al. 1958), and in many other bacteria (Jun et al. 2018). In *S. typhimurium* and *E. coli*, there is a ~ 5 -fold increase in cell volume over the full range of growth rates (Volkmer and Heinemann 2011; Si et al. 2017), whereas the full response in the photosynthetic cyanobacterium *Synechocystis* is a 1.5-fold increase in cell volume (Zavřel et al. 2019).

A positive relationship between cell volume and nutrient status has also been documented in unicellular eukaryotes. For example, the ciliate *Tetrahymena* exhibits a two-fold increase in cell volume with nutrient availability (Zalkinder 1979), and the budding yeast *S. cerevisiae* (Tyson et al. 1979; Ferrezuelo et al. 2012) and the green alga *Chlorella pyrenoidosa* (Prokop and Ricica 1968) both have five-fold ranges. Given this near-universality of the positive physiological response of cell volume to nutrient availability, it too has often been christened as a “growth law.”

What remains unclear is the extent to which this kind of cell size-growth rate relationship is driven by adaptive processes, i.e., whether increasing cell volume under high nutrient conditions somehow enhances the cell-division rate beyond that expected under constant cell size. Although it is certainly unlikely that such a universal response is maladaptive, an argument is made below as to how, under the adder model, cells phenotypically shifted to larger sizes might passively accumulate in cultures growing with higher rates of cell division.

Equally unclear is the degree to which the purely physiologically driven cell size-growth relationship associated with resource availability noted here is related to the phylogenetic association between cell size and maximum-growth rate outlined in the preceding chapter (Figure 8.5). On the one hand, the positive association between maximum cell-division rate and cell size among heterotrophic bacterial species is consistent with the developmental-plasticity pattern. Also consistent with this pattern is a long-term selection experiment for higher growth rate in *E. coli*, which yielded a parallel response in cell volume (Figure 9.5). On the other hand, among eukaryotic species, maximum cell-division rates decline with increasing cell size (Figure 8.5), contrary to within-species responses to a shift in nutrient availability (Figure 9.7A).

Why is there a conflict between responses at the evolutionary and physiological levels in eukaryotes but not in prokaryotes? One possibility is that, despite retaining the physiological downshift in size under low-nutrient conditions, evolution of the maximum growth capacity of eukaryotic cells with increasing size is compromised owing to the reduction in efficiency of natural selection imposed by the increased power of random genetic drift (Chapter 8). By extension, if this hypothesis is correct, small- to moderate-sized bacterial species should retain the flexibility to jointly evolve large cell size and high growth rates (Figure 9.6), whereas eukaryotic cells should be much more constrained.

Finally, we consider the effects of temperature, one of the most widely varying environmental parameters influencing cell physiology. Membrane fluidity, diffusion coefficients, and essentially all biochemical reaction rates (within the bounds of protein stability) increase with increasing temperature (Chapter 7). Given the positive association between cell size and growth rate in constant-temperature environments, one might expect that higher temperatures would promote both faster growth (within physiological limits) and larger cell volumes. Unfortunately, there is remarkably little information on this matter in prokaryotes, although in their seminal work, Schaechter et al. (1958) found that *Salmonella* cells grown at low

temperature are substantially larger than those growing at identical rates (with lower nutrients) at higher temperatures. Their results suggest that temperature induces a different cell-size response to growth rate than does nutrient availability – to maintain a specific growth rate at lower temperatures, individual cells seemingly have to be larger (Figure 9.7B).

How generalizable is this sort of observation? Although there is a long history of thought on the relationship between organism size and temperature, the focus has mostly been on multicellular species. Here, the general idea is that organisms living in cooler environments have larger body sizes (within and among species), ostensibly because reduced surface area:volume ratios mitigate heat loss. This pattern has come to be known as Bergmann’s rule, in honor of the originator of the idea (Bergmann 1847). Although its generality has come to be questioned for multicellular organisms (Riemer et al. 2018), the expected pattern does appear to hold for microbial eukaryotes, albeit likely for different reasons than proposed for homeothermic vertebrates. In every study where the matter has been closely investigated, average cell volume declines with increasing temperature, while the growth rate increases. Such observations have been drawn from ciliates, flagellates, amoeboid heterotrophs, and diverse phototrophs, with the average response being an $\sim 25\%$ decrease in cell volume accompanying a 10°C increase in temperature (Atkinson et al. 2003; Fu and Gong 2017; Zohary et al. 2020). If nothing else, such observations demonstrate that the positive association between cell size and growth rate found in different nutritional environments is not generalizable to other environmental effects.

Again, whereas such a universal temperature response among diverse unicellular species might suggest the need for a general adaptive explanation for such behavior, the basis for such patterns remains unclear. Indeed, given the existence of size-selective predation and potential size-associated competitive interactions and physical-environmental effects, mortality rates are likely to be size-dependent, so it is by no means clear that induction of large cell size is uniformly favorable in colder natural environments.

Is the physiological response to temperature change, running in the opposite direction to that induced by nutritional differences, an unavoidable by-product of the molecular mechanisms that set times to division? Future work in this area should look to the numerous experiments showing that when the translational capacity of ribosomes is compromised by chemical manipulation in *E. coli*, the phenotypic scaling between cell size and growth rate runs in opposite directions to the nutrient-based pattern (Scott et al. 2010; Jun et al. 2018; Serbanescu et al. 2020). Perhaps the same underlying mechanism applies to temperature shifts.

Scaling of Intracellular Features

It is well known that various organs, tissues, and other body parts scale with body size as multicellular organisms grow (Thompson 1917), a phenomenon known as developmental allometry. Less clear is the extent to which internal cellular features (including transcript and protein numbers, organelle numbers and size, etc.) scale as cells grow from birth to maturity. A general positive relationship between levels of

cellular components and cell volume can be expected, as the organelles and molecular constituents of cells have functional roles whose total demands typically increase with the volume of cell. However, the expected quantitative patterns of scaling are less clear.

On the one hand, intracellular features might scale isometrically throughout growth (thereby keeping the intracellular environment relatively constant). Such scaling would be consistent with the exponential growth in cell volume noted above, which implies the maintenance of constant growth capacity per unit cell volume regardless of cell size. On the other hand, as cells grow and experience reductions in the surface area : volume ratio, the effective availability of nutrients per unit biomass might be reduced. If so, altered investments in the machinery associated with nutrient uptake and intracellular transport may be required, much like the responses of ribosome investment seen when cells are grown under different nutrient conditions.

For the few eukaryotic cellular traits with a modicum of data, isometric scaling with cell volume appears to be the norm. For example, in yeasts, mitochondrial volume constitutes $\sim 1\%$ of cell volume throughout life in *S. cerevisiae* (Rafelski et al. 2012), $\sim 10\%$ in *Candida albicans* (Tanaka et al. 1985), and $\sim 9\%$ in *Cryptococcus neoformans* (Mochizuki et al. 1998). Isometric scaling is also true in HeLa cells, with $\sim 10\%$ of the fractional volume of consisting of mitochondria (Posakony et al. 1977). Throughout growth in *Euglena gracilis*, the plastid constitutes $\sim 16\%$ and the mitochondrion $\sim 6\%$ of the total cell volume (Pelligrini 1980). Likewise, in the green alga *Chlorella fusca*, the volumetric contributions of plastids, mitochondria, and vacuoles remain nearly constant, at 40, 3, and 10% respectively (Atkinson et al. 1974). Total vacuole volume also scales nearly isometrically in *S. cerevisiae*, constituting $\sim 6\%$ of cell volume throughout the cell cycle (Chan and Marshall 2014; Chan et al. 2016). On the other hand, the essentially linear actin cables in yeast appear to scale with the length of the cell (McInally et al. 2021).

Compelling evidence for active cell-volumetric control of organelle size derives from observations on the eukaryotic nucleus. In both *S. cerevisiae* and *S. pombe*, nuclear volume comprises a nearly constant ~ 6 to 8% of cell volume throughout cell growth (Jorgensen et al. 2007; Goehring and Hyman 2012). Transplants of nuclei from small to large cells reveal that the nucleus expands to the size expected given the host-cell volume. Such responses are not affected by the amount DNA in the nucleus, as they are even observed when DNA content is increased as much as 16-fold (Neumann and Nurse 2007). Similar responses have been seen in vertebrate cell cultures (Levy and Heald 2012), and it appears that the nuclear-to-cytoplasmic volume ratio is largely governed by a simple balance of osmotic pressures associated with the numbers of protein molecules in the nucleus vs. the cytoplasm (Deviri and Safran 2022; Lemièrè et al. 2022). Notably, across a wide range of prokaryotic species, the size of the nucleoid (the amorphous region of the genome, without nuclear envelopes or histone-packaging of chromosomes) also grows nearly isometrically with cell volume within the growth cycle (Gray et al. 2019).

Although the molecular mechanisms underlying cytoplasmic-composition homeostasis throughout the cell cycle remain mostly unknown (Chan and Marshall 2010, 2012; Goehring and Hyman 2012; Brangwynne 2013), the emerging picture is that cells typically operate as bioreactors, with relatively constant internal compositions,

until rapid remodeling takes place at the time of division. Still, this leaves open the question as to whether individual cellular features grow independently through time at roughly the same rate, or are somehow mutually guided via feedback associated with cell volume. These two alternative models make somewhat different predictions with respect to scaling relationships (Foundations 9.3). Passive homeostasis might simply arise from global changes in transcription rates in response to growth rate, thereby leading indirectly to coordinated assembly of subcellular compartments without the need for elaborate system-specific regulatory mechanisms.

It is also unclear how the ontogenetic patterns noted here relate to among-species scaling patterns observed at the phylogenetic level (Chapter 8). Returning to the questions relating to cell size and growth rate in the previous section, are the prevailing statistical relationships seen between pairs of characters during development recapitulated over evolutionary time with the divergence of phylogenetic lineages, or can evolution promote shifts in cellular composition in arbitrary directions? An organism's repertoire of developmental and phenotypic plasticities sets the range of phenotypic combinations that can be achieved and tested by natural selection prior to genetic change, so in principle genetic alterations that simply hardwire a plastic response into a constitutively expressed phenotype may provide a readily accessible route to multivariate evolution. This very old idea (Baldwin 1896; Waddington 1942) essentially suggests that natural selection will typically exploit the paths of least resistance by genetically assimilating preexisting possibilities. Such a view is not very different than the conventional vision of evolution as a process of descent with modification.

If this is the case for intracellular architecture, then the observations noted above suggest that isometric scaling of eukaryotic cell parts should also prevail at the phylogenetic level. Although the topic is largely unexplored, the kinds of phylogenetic scalings outlined in Chapters 7 and 8 provide compelling material for future investigation. Indeed, with its strong molecular basis, evolutionary cell biology provides a compelling platform for understanding the mechanistic links (or lack thereof) between allometric scaling relationships at the ontogenetic (developmental), environmental (physiological), and phylogenetic levels.

Phenotypic Variation in Cell Size and Division Time

Although the preceding discussion has focused largely on the average behavior of cell-growth features, the stochasticity of events inherent in growth-related processes generates nontrivial variation in cell traits (Geiler-Samerotte et al. 2013). Sources of variation for cell size and growth rate include: 1) variation in birth size owing to imperfect partitioning at cell division; 2) variation in numbers of ribosomes and of other critical molecules per cell, partly associated with variation in initial partitioning, but also from subsequent events such as transcription and translation; 3) inaccuracies in the growth-increment target; and 4) extrinsic variation in the microenvironment.

Many attempts have been made to incorporate one or more of these factors into models of steady-state distributions of cell size and division time (e.g., Powell 1956; Scherbaum and Rasch 1957; Koch and Schaechter 1962; Tyson and Hannsgen

1985a,b; Taheri-Araghi et al. 2015; Jun et al. 2018). There is by no means uniformity in opinion on the mathematical forms of cell-feature distributions, and the details will not be pursued here. However, it is worth noting that predicted patterns are often closely related to formal distributions derived in the early days of statistics for entirely different reasons. For example, the Yule (1925) distribution can be used to describe situations involving parallel (autonomous) growth of cellular constituents, such that cell parts are duplicated during the cell-growth process, with each duplication occurring independently with fixed probability per unit time, and cell division occurring at the time of duplication of the final part. In contrast, a Pearson Type III distribution describes a situation in which cell division takes place only after the completion of a series of consecutive (interdependent) steps, with each initiated step completed with a certain probability per unit time following the exit from the preceding step (Kendall 1948). Although these models do not strictly incorporate variability in size at birth, they do have features that are conceptually connected to the assumptions under the adder model, where a certain amount of cellular biomass must accrue before the cell divides. They also generate skewed distributions with long tails to the right, superficially similar to what is typically seen with real data (Figure 9.8).

Results from single-cell monitoring demonstrate that the magnitude of standing variation among genetically uniform cells is generally quite large. Observations from well-mixed laboratory cultures of unicellular species commonly yield coefficients of variation (CVs, equal to the standard deviation divided by the mean) in the range of 0.1 to 0.5 for size at birth and maturity, incremental addition, and age at division (Table 9.1). As all of the studies in Table 9.1 involve single genotypes, the observed variance is due entirely to vagaries in the internal and external cellular environment. Yet, CVs of this magnitude are substantially greater than those observed for morphometric traits in genetically variable samples of multicellular organisms, which are usually on the order of 0.05 to 0.10 (Lynch and Walsh 1998).

Owing to bursty transcription and translation (Rhee et al. 2014; Cao and Grima 2020; Chapter 21), high levels of cell-to-cell variation extend to the molecular level, and this likely feeds back in ways that contribute to variation in cell life-history traits. For a diversity of prokaryotes and eukaryotes, the CV for the number of molecules of particular proteins scales as $\bar{z}^{-0.2}$, where \bar{z} is the mean number of proteins/cell (Vallania et al. 2014). As the average number of protein molecules per genetic locus per cell ranges from 10 to 10^5 from the smallest to the largest cell types (Figure 7.4), this implies CVs $\simeq 0.6$ to 0.1, with some evidence suggesting that 0.1 may be close to the asymptotic lower limit for highly expressed proteins (Keren et al. 2015). The CV for protein numbers also increases with decreasing cell-division rates by a factor of ~ 3 over the whole range of growth rates (Keren et al. 2015).

Table 9.1. Coefficients of variation (CV, standard deviation divided by the mean) for growth-related features of cells.

Species	Trait	CV	Reference
Bacteria:			
<i>Aerobacter cloacae</i>	Generation time	0.18	Powell 1958

<i>Azotobacter agilis</i>	Elongation rate	0.10	Harvey et al. 1967
	Generation time	0.22	Harvey et al. 1967
<i>Bacillus mycoides</i>	Generation time	0.48	Powell 1956
<i>Bacillus subtilis</i>	Generation time	0.54	Powell 1956
<i>Bacterium aerogenes</i>	Generation time	0.30	Powell 1956
<i>Escherichia coli</i>	Elongation rate	0.08	Taheri-Araghi et al. 2015
	Division length	0.14	Taheri-Araghi et al. 2015
		0.12	Harvey et al. 1967
	Birth length	0.16	Taheri-Araghi et al. 2015
	Generation time	0.21	Taheri-Araghi et al. 2015
		0.28	Harvey et al. 1967
		0.30	Kiviet et al. 2014
	Added length	0.24	Taheri-Araghi et al. 2015
<i>Proteus vulgaris</i>	Generation time	0.32	Powell 1956
<i>Pseudomonas aeruginosa</i>	Generation time	0.14	Powell 1958
<i>Serratia marcescens</i>	Generation time	0.17	Powell 1958
	Generation time	0.14	Tyson 1989
<i>Streptococcus faecalis</i>	Generation time	0.27	Powell 1956
Eukaryotes:			
<i>Saccharomyces cerevisiae</i>	Length of G1 phase	0.46	Di Talia et al. 2007
<i>Schizosaccharomyces pombe</i>	Division length	0.07	Tyson 1989
<i>Tetrahymena pyriformis</i>	Generation time	0.12	Scherbaum and Rasch 1957
	Division size	0.12	Scherbaum and Rasch 1957

Stochastic partitioning of cell contents at division. In most studies of variation in multicellular organisms, the relative contributions of different causal sources of variation are unknown (Lynch and Walsh 1998). However, for cellular traits, a number of insights can be gained from first principles. We start with the ways in which the basic features of molecular segregation during cell division generates variation among progeny. Such stochastic inheritance can have an equally if not greater overall effect than intrinsic transcriptional noise (Chapter 21) for the simple reason that upstream variation in molecular abundance can further generate downstream gene-expression noise, and vice versa. Such an outcome is a simple consequence of the structure of biology – numerous cellular products are responsible in one or more ways for their own production (Kiviet et al. 2014).

For the simplest case of a cell containing n molecules at the time of division, with each being independently and randomly distributed to the two daughter cells with probability $1/2$, the average number of molecules inherited per offspring cell is $\bar{n}_o = n/2$, but from the binomial sampling formula the variance (i.e., the square of the standard deviation) is $\sigma_{n_o}^2 = n(1/2)(1/2) = n/4$. The coefficient of variation is then $CV(n_o) = \sigma_{n_o}/\bar{n}_o = 1/\sqrt{n}$, showing that relative to the mean, the standard deviation is inversely related to the square root of the number of molecules being partitioned. This simple principle predicts elevated CVs in small cells containing smaller numbers of molecules. It may also, in part, explain the reduction in CVs in traits in multicellular species, which might average out the noise from their constituent cells.

Additional sources of stochastic inheritance during cell division can inflate the level of variation further. The argument outlined in the previous paragraph assumes the ideal situation in which each daughter cell draws from an identical cytoplasmic pool. If, however, the cell volumes of daughter cells are unequal (owing to the

imperfect positioning of the division septum), the coefficient of variation for offspring cells increases to

$$\text{CV}(n_o) = \left(\frac{1 - [\text{CV}(V)]^2}{\bar{n}} + [[\text{CV}(V)]^2 \cdot \{[\text{CV}(n)]^2 + 1\}] \right)^{0.5}, \quad (9.9)$$

where \bar{n} is the average number of molecules per adult cell, and $\text{CV}(V)$ and $\text{CV}(n)$ are, respectively, the coefficients of variation for offspring (sister-cell) volume and for the number of molecules per parental cell (Huh and Paulsson 2011). Empirical estimates of $\text{CV}(V) \simeq 0.05$ to 0.12 in *E. coli* (Trueba 1982), *Bacillus subtilis* (Nanninga et al. 1979), *Caulobacter crescentus* (Trueba 1982), and *Schizosaccharomyces pombe* (Johnson et al. 1979; Tyson 1989). $\text{CV}(n)$ is typically of similar magnitude to that for $\text{CV}(V)$ and relatively similar among species, $\simeq 0.10$ in *E. coli* (Schaechter et al. 1962; Harvey et al. 1967), *Azotobacter agilis* (Harvey et al. 1967), and *Salmonella typhimurium* (Schaechter et al. 1962), and 0.16 in the dinoflagellate *Gonyaulax polyedra* (Homma and Hastings 1989), and 0.07 in the yeast *S. pombe* (Tyson 1989).

Unless $\bar{n} < 100$, with $\text{CV}(V)$ and $\text{CV}(n)$ both < 0.1 , it can be seen from Equation 9.9 that random partitioning of cell volume does not greatly elevate the level of variation in the inherited numbers of molecules beyond the binomial expectation, $1/\sqrt{\bar{n}}$. On the other hand, if $\text{CV}(V) > 0.1$, the inflation can be greater than tenfold with small \bar{n} (Figure 9.9).

Eukaryotic cells have an additional layer of stochasticity in that some molecules are segregated into vesicles or organelles prior to cell division, which are then randomly partitioned among offspring cells. Huh and Paulsson (2011) provide a general expression for the variation rendered under this model. If it assumed that the numbers of vesicles per cell are independently distributed, and that the molecules are randomly distributed among vesicles,

$$\text{CV}'(n_o) \simeq \left(\frac{1}{\bar{n}} + \frac{\{1 + [\text{CV}(n_o)]^2\}\{1 + [\text{CV}(v)]^2\}}{\bar{v}} \right)^{0.5}, \quad (9.10)$$

where \bar{v} and $\text{CV}(v)$ are the mean and coefficient of variation of the number of vesicles per cell. From Equation 9.9, we know that $\text{CV}(n_o) > 1/\sqrt{\bar{n}}$ and possibly as large as 10. Studies of mitochondrial inheritance in the fission yeast *S. pombe* (Jajoo et al. 2016) and of endosome inheritance in mammalian cell cultures (Bergeland et al. 2001) suggest that the partitioning of such organelles is only slightly less variable than the binomial expectation, which would imply $\text{CV}(v) \simeq 1/\sqrt{\bar{v}}$. In addition, we expect the mean number of vesicles (\bar{v}) to be much lower than the mean number of molecules (\bar{n}) per cell.

Thus, it is clear that the stochastic partitioning of vesicles (described in the second fraction in Equation 9.10) can be a dominant source of intracellular variation unless there is some regulatory mechanism for controlling cargo partitioning among vesicles and vesicle partitioning among offspring cells. Moreover, variable organelle partitioning is likely to generate more phenotypic variation among cells than might be expected based just on organelle number. For example, because mitochondria are the sites of ATP production in eukaryotic cells, and ATP drives transcription and other cellular processes, mitochondrial partitioning during inheritance can have

nonadditive effects on offspring cell performance (das Neves et al. 2010; Johnston et al. 2012).

Finally, it is worth noting that some cellular features can lead to a less variable pattern of inheritance of intracellular contents than expected by chance. For example, in *E. coli* (and many other bacteria) the genome is compacted into a centrally located nucleoid. The resultant mesh-like features serve as a barrier to the movement of ribosomes, which then become more concentrated towards cellular poles for purely physical reasons (Castellana et al. 2016). This may lead to a more even distribution of ribosome numbers in progeny cells than expected if each ribosome were drawn independently.

Phenotypic Variation and Adaptation

As explained in prior chapters, not all of evolutionary change is a product of natural selection, and as adaptive as they might seem superficially, certain kinds of changes can only be efficiently promoted by selection under a narrow range of population-genetic conditions. Nonetheless, either unaware or unconvinced of such issues, numerous investigators have asserted that variation-inducing features, like those noted above, are not simple consequences of biophysical constraints, but have been advanced by natural selection as strategies for survival in variable environments. In reality, however, there is a remarkable void of evidence for phenotypic variance (aside from regulated phenotypic plasticity) serving an adaptive purpose, and good reasons to think otherwise.

The following provides an overview of the general consequences of phenotypic variation for the process of natural selection. First, we consider how nonheritable environmental noise, such as that induced by cellular stochasticity, reduces the response to selection on a trait by obscuring the genetic differences among members of a population. Second, we demonstrate how, even in the absence of genetic variation, selection can yield a transient (and in some cases persistent) change in the phenotypic properties of a cell lineage, provided the environmental deviations among individuals are at least partially heritable, as will often be the case for growth-related traits. Finally, we will return to the issue of whether phenotypic variation (within genotypes) is maintained by natural selection as a mechanism for coping with a variable environment.

Environmental variation and the efficiency of selection. One of the bedrock results of evolutionary theory concerns the nature of the underlying determinants of the resemblance between relatives. Understanding this issue is critical to understanding processes of adaptation for a very simple reason. Although the process of natural selection will always proceed provided there is fitness-associated phenotypic variation is present, only the fraction of variation with a heritable genetic basis is relevant to permanent evolutionary change. As will be shown in the following section, heritable environmental effects can lead to some response to directional selection, but any such response is transient, quickly decaying away once the prevailing selection pressure is terminated.

The central question here is the degree to which offspring phenotypes resemble

those of their parents. For asexually reproducing cells, this is simply defined by the fraction of the phenotypic variation that is genetic in basis, a quantity known as the broad-sense heritability (or H^2) (Foundations 9.4). This key measure is readily estimated by taking a random sample of a population and regressing offspring on parental phenotypes (Lynch and Walsh 1998). The best-fit slope, which is generally restricted to the range of 0.0 to 1.0, is equivalent to H^2 (Figure 9.10). Because total phenotypic variance is the sum of contributions from genetic and environmental effects, the higher the background noise from environmental causes, the lower the heritability of the trait.

The heritability of a trait is, in turn, directly related to the response to selection. Imagine a parental population with phenotypic mean \bar{P}_p prior to selection, with directional selection then moving this to \bar{P}'_p , yielding a change of $S = \bar{P}'_p - \bar{P}_p$. This difference S in mean phenotypes prior to reproduction is called the selection differential. As an example, Figure 9.10 shows a situation in which an initial phenotype distribution (black bell-shaped curve) is shifted to the right by viability selection (red curve). The diagonal line denotes the parent-offspring regression. If there were perfect transmission of phenotypes across generations, i.e., if $H^2 = 1$, the mean offspring phenotype would be identical to that of the selected parent generation, and the response to selection (R) would equal the selection differential. However, if there is environmental variance for the trait, the slope of the parent-offspring regression will be < 1 , and transmission will be less than perfect because the parental phenotypes deviate from their underlying genotypic values. This is often referred to as regression towards mediocrity. If there is no genetic variation, there will be no permanent selection response at all.

Summing up, for a population of asexually reproducing cells, the response to selection is simply

$$R = H^2 S, \quad (9.11)$$

showing that H^2 is equivalent to the fraction of the selection differential that is transmitted across generations. In a simple fashion, this result illustrates that the ability of natural selection to promote genetic change declines with increasing environmental variation.

Inheritance of environmental effects. Although a permanent response to directional selection requires the promotion of underlying genetic change, a transient response can sometimes be achieved in the absence of genetic variation. Because selection operates regardless of the source of phenotypic variation, if variation at the phenotypic level owing to intrinsic and/or extrinsic environmental effects is partly heritable across generations, the mean phenotype will still move in the direction of selection, even in the absence of genetic variation (Foundations 9.5). However, unlike the situation with genetic change, such a shift will not be permanent. Rather, under persistent directional selection, the population mean phenotype is expected to reach an alternative steady state reflecting a balance between the directional force of selection operating on phenotypes and the erosion of progress each generation resulting from the dilution of inherited environmental effects. If selection is relaxed, all progress due to the inheritance of acquired environmental deviations will be quickly eroded away.

This sort of transient response to selection applies to any cellular feature that is partly inherited across generations. For example, any trait that is a function of the number of molecules within a cell (such as a metabolic rate) will naturally be subject to inheritance across cellular generations owing to the fact that the contents of progeny cells are derived immediately from parental-cell constituents, with the molecular composition subsequently undergoing turnover associated with continued production and degradation. Given that offspring in unicellular species inherit half of their parent-cell constituents, these kinds of effects are expected to be much more significant than in multicellular species. Indeed, the complete dissipation of maternal environmental effects can require up to ten generations in bacterial populations (Vashistha et al. 2021).

Such effects are of likely relevance to laboratory experiments that either intentionally or indirectly select for extreme phenotypes. For example, as noted above for the adder growth model, large adult cells yield large progeny cells (although not as large, on average, as themselves), which more rapidly reach the point of cell division. Smaller cells take a longer time to reach the requisite cell-volume increase of Δ , and hence lag in terms of their contribution to the growing population. Although the descendants of large, rapidly dividing cells will gradually move back towards the expected offspring size of Δ , with imperfect cell division, extreme cell sizes will continuously be produced anew, recreating the biasing process. This verbal model needs to be worked out in a more formal manner, but it provides a potentially simple and general explanation for the consistent observation of cells becoming larger in environments with higher nutritional status, even in the absence of genetic variation, as noted above.

A selection experiment by Yoshida et al. (2014) may be relevant here. Using a cell sorter, they selected for smaller cell size in cultures of *E. coli* for 22 consecutive days by allowing only the smallest 1% of reproducing cells to propagate to the next generation. Overall, an $\sim 20\%$ decline of mean cell size was observed, with the variance in size decreasing only slightly (implying that sufficient opportunity for selection, but not necessarily genetic variance, remained throughout the experiment). Sequencing the entire genome of one selected population revealed only a single nucleotide change, the relevance of which remained unclear.

Although the logic just outlined provides a simple argument for why one expects an elevated resemblance between parents and offspring associated with transiently heritable environmental effects, there has been some suggestion of an even higher correlation between collateral relatives (i.e., relatives that are not direct descendants) within genetically uniform cultures of cells. For example, Sandler et al. (2015) found that the correlation between cell-division times in parent and offspring lymphoblast cells is just 0.04, whereas that between sister cells is 0.71, and that between first-cousins is 0.58. They call this elevated correlation among cousins relative to that between mother and offspring cells the “cousin-mother inequality.” Cultures of mammalian cancer and embryonic stem cells exhibit similar behavior (Froese 1964; Kuchen et al. 2020).

These kinds of observations have also been made with cell-lineage studies of several bacterial species (Powell 1958). For example, in *Aerobacter cloacae*, the correlation in cell-division time is -0.15 for mother-daughter cells, but 0.44 for sibs, and 0.19 for first cousins. Likewise, for *Serratia marcescens*, these correlations are,

respectively, -0.20, 0.58, and 0.38. The reduced correlation between first cousins relative to that between sibs is consistent with a progressive dilution of shared effects, and as expected, an even further decline is observed for second cousins (Powell 1958).

Superficially, these results suggest a mechanism of inheritance that is lost for one generation, and then regained in the next, with subsequent erosion of the correlation occurring among the parallel descendants of maternal lineages. This led to the claim that such reappearance of heritability cannot be explained by stochastic inheritance, and requires an underlying deterministic mechanism (Pearl Mizrahi et al. 2015; Sandler et al. 2015). However, although a model can be set up in which an internal oscillator (putatively a circadian clock) operates with a periodicity such that first cousins are born at approximately the same time (Sandler et al. 2015), the following simple argument indicates that a deterministic mechanism need not be invoked.

Imagine that parent cells have their division times determined by physiological effects experienced early in life, but that en route to division, additional resources are gained (or lost) that will influence the division times of their offspring, e.g., a burst of transcriptional/translational activity late in the maternal cell cycle. Upon fission, these resources will then be approximately equally allocated to the two progeny cells, causing a sib correlation in the population, but having little effect on the maternal-offspring correlation. Although sibs share maternal effects, only a fraction of these will be transmitted to the next generation (leading to a smaller first-cousin correlation, and a still smaller one for second cousins) (Staudte et al. 1996).

The adaptive value of phenotypic variation. Finally, we turn to the common argument that within-genotype phenotypic variation is molded by natural selection to provide a strategy for dealing with environmental variation (Thattai and van Oudenaarden 2004; Kussell and Leibler 2005; Fraser and Kaern 2009; Eldar and Elowitz 2010; Zhuravel et al. 2010; Kiviet et al. 2014; Ackermann 2015; Jahn et al. 2015). As already noted, cellular features exhibit substantial, unavoidable variation owing simply to the intrinsic stochasticities of cellular processes. Here, we note several compelling theoretical reasons for why the further promotion of variation by selection should be the exception rather than the norm. The focus here is not on major discrete phenotypic changes induced by environmental triggers (such as spore formation, or transition to motility), which in many cases almost certainly represent adaptive survival mechanisms (Wolf et al. 2005; Losick and Desplan 2008). Rather, the question is whether the continuous range of variation typically associated with quantitative traits such as growth rate, cell size, and metabolic rates constitutes an adaptive bet-hedging strategy.

One of the most substantive reasons for questioning assertions about adaptive maintenance of phenotypic variation relates to the fact that selection is agnostic with respect to the underlying genetic/environmental determinants of variance. Following the logic outlined above, if selection favors an extreme phenotype, when individuals at the extreme are largely there as a consequence of nongenetic effects, the ability of selection to promote individuals with a genetic predisposition to extreme trait values will be compromised. This is because individuals with particularly extreme genetic values will compete for promotion by natural selection with those with more

average genetic values but higher variance in expression (Bull 1987). Thus, selection for variance-producing genotypes is difficult when levels of stochastic phenotypic variance are already high. The likelihood of success is even lower if individuals with extreme genetic values have narrower conditional phenotype distributions around the expectation, as these would then be more visible to natural selection.

Of related importance is the fact that selection on phenotypic variation is a second-order effect, as individual genotypes are not promoted on the basis of their own expected genotypic values but via the distribution of their descendants' phenotypes. Unless there is continuing fluctuating selection for individuals at the opposite phenotypic extremes at a sufficiently high rate, the link between genotypic fitness and the ability to differentially generate variation will be weak. This will especially be the case for sexually reproducing species where recombination will progressively remove the disequilibrium between parental genotypic values and descendant phenotype distributions.

Although these arguments do not entirely rule out the possibility of direct selection for the production of broad phenotype distributions, they do lay out the substantial logical challenges confronting those who wish to invoke the existence of phenotypic variation as a direct product of adaptation. It is one thing to hypothesize on the optimality of a complex feature, but quite another to demonstrate that natural selection is actually capable of advancing such change.

As a more explicit example of interpretative difficulties here, consider a study in which single-cell monitoring methods were used to demonstrate that the rate of exponential growth of a culture of *E. coli* with the same average cell-division time is elevated if there is variance around the mean (Hashimoto et al. 2016). The authors argued that these results demonstrate a “fundamental benefit of noise for population growth.” However, as we know that the rate of population expansion (r) is inversely related to cell doubling time (t_D) (Equation 9.2), this result was readily predictable in advance – for any absolute change in t_D , the increment in r with decreased t_D is greater than the decrease incurred with increased t_D . The behavior results simply because in a growing population, r is bounded above 0.0 and increases at an accelerating rate as t_D becomes small. No elaborate experiment was necessary to show this.

On the other hand, the outcome would have been completely different if the population was declining rather than increasing. In this case, a sublineage of cells with an absolute deviation in division time below the average will experience a greater change in the rate of decline than will a sublineage with a positive deviation of the same absolute amount. Here, variation in the underlying trait enhances the rate of decline of the sublineage. This is not a trivial example for the simple reason that, on average, populations ultimately must go through equal periods of growth and decline, else the population will either go extinct or fill the universe.

More generally, the relationship between the level of variation and the expansion of growth of a cell lineage can be seen to be a simple consequence of the form of the fitness function (Figure 9.11). If the relationship between phenotype and fitness is concave upward, the average fitness of a variable population will be greater than that of a population having the same mean phenotype but no variance. In contrast, if the fitness-phenotype relationship is concave downward, the opposite occurs – in this case, the boost in fitness from the upwardly deviating phenotypes is smaller

than the loss of fitness in downwardly deviating phenotypes. An extreme case can be seen for the situation in which the trait is under stabilizing selection with the mean phenotype coinciding with the optimum – any deviation from the optimum will result in a decline in fitness. Only for the special situation in which the fitness function is perfectly linear is the influence of variation on fitness effectively neutral, owing to the fact that equal upward and downward phenotypic deviations have equivalent effects on fitness.

Finally, even these arguments are not ironclad, as they consider only the situation in which the phenotype distribution is symmetrically distributed about the mean. With asymmetric phenotype distributions, many alternative outcomes are possible, as the bulk of the phenotype distribution may reside in regions where the fitness function is either increasing or declining. The salient issue is that there is no general advantage to phenotypic variation. Although transient situations may arise in which variation is useful, the same may be said for periods in which it is detrimental.

The general conclusion then is that intrinsic variation in cellular processes results in high levels of phenotypic variation among individual cells, much higher than observed among individuals in multicellular species. As seductive as it is to attach an adaptive meaning to all things biological, the idea that phenotypic variance is generally promoted by selective processes appears to be a substantial overstatement if not positively misleading. The very structure of biology makes the avoidance of phenotypic variation impossible.

Summary

- Observations from a diversity of organisms reveal a number of patterns involving cellular responses to growth environments that are general enough to be labeled “growth laws” by microbial physiologists. One universal relationship is the increase in relative investment in ribosomes with increasing cell-division rate, reflecting the conflict of the high energetic cost of ribosomes and their necessity for building cellular material.
- The response of cell-division rate to the concentration of a limiting nutrient can generally be described by a hyperbolic function similar to the Michaelis-Menten form for enzyme kinetics.
- The growth of cell volume within a cellular life cycle is typically exponential in form, as expected if reaction rates per cytoplasmic volume are nearly size-independent. Consistent with this view, the ontogenetic response of cell composition to cell volume during individual growth appears generally to be isometric, such that the relative proportions of cell contents remain constant.
- A wide array of prokaryotic and eukaryotic cells determine their division times by monitoring the total change in size, rather than by targeting a specific size or

time, dividing only after a threshold amount of material has been added. Such behavior naturally leads to cell-size homeostasis.

- The models for such growth patterns serve as first-order approximations and are phenomenological in nature, as the underlying mechanisms driving them remain uncertain and are variable among species. Nonetheless, evidence suggests that the determination of growth-size thresholds often involve the products of just two or three genes, implying relatively simple evolutionary paths for altering cell size and division time.
- In all species that have been studied closely, cell size increases with the nutrient status of the environment, but decreases with increasing temperature. It remains unclear whether such shifts are adaptive in any way. They may simply be inevitable by-products of the underlying molecular mechanisms by which cells commit to division.
- Numerous sources of stochastic variation, ranging from sporadic transcription / translation to random partitioning of cellular contents at division, result in considerable phenotypic variation among genetically identical cells, even in well mixed environments. The magnitude of such variation, which obscures the visibility of genetic differences to natural selection, is substantially greater in unicellular than in multicellular organisms.
- Owing to the fact that binary fission results in substantial sharing of the contents of parent, offspring, and sib cells, unicellular lineages are subject to significant inheritance of nongenetic effects, which can lead to transient shifts in phenotypic values in the absence of genetic change.
- Although there has been considerable speculation that the tendency to produce such high levels of phenotypic variation has been advanced by natural selection as means for coping with variable environments, there is little empirical or theoretical support for this contention.

Foundations 9.1. The scaling of ribosome number and cell growth rate.

Although cells in nature commonly experience fluctuations in resource availability on time scales shorter than the cell-division time, it is instructive to consider the steady-state situation in a constant environment, as when cells are grown in a continuous-flow chemostat (Chapter 8). Under such conditions, the production rate of every biomolecule (per existing molecule) in the cell must be identical to the rate of overall cell growth, ensuring a steady-state cellular composition.

The rate of translation per cell, and hence the cellular growth rate, ultimately depends on the number of ribosomes and the number of mRNA transcripts that they encounter. Although translation also involves the use of accessory proteins (e.g., aminoacyl tRNA synthetases, elongation factor, and many others; Barenholz et al. 2016) and transfer RNAs, the abundance of such factors under steady-state growth will be in constant proportion to that of the ribosomes, leaving the latter as a quantifiable indicator of the rate of translation, and hence cell growth. This argument assumes that cells are conservative with respect to the production of energetically expensive ribosomes, i.e., produce no more than needed to service the current mRNA pool. Here, we follow a derivation presented by Scott et al. (2010) to quantify this connection.

Letting M denote the total protein mass associated with a cell, and M_R denote the total protein mass associated with ribosomes and their affiliated proteins, i.e., “extended ribosomes,” then $f_R = M_R/M$ is the fractional allocation of proteins to translation. Letting m_R denote the protein mass of a single extended ribosome, which will hereafter be simply abbreviated to ribosome, the number of ribosomes per cell is $N_R = M_R/m_R = f_R M/m_R$.

Assuming that all ribosomes are engaged in translation, letting k_T denote the rate of translation (i.e., the rate at which amino acids are added to elongating protein chains, here assumed to be constant), and letting m_{AA} be the average mass of an amino acid, the rate of increase in cellular protein mass is

$$\frac{dM}{dt} = m_{AA} \cdot k_T \cdot N_R = \left(\frac{m_{AA} \cdot k_T \cdot f_R}{m_R} \right) \cdot M. \quad (9.1.1a)$$

Because the mass of all components of the cell must increase at the same rate under steady-state conditions, and cell division must proceed at the same rate as growth in size, Equation 9.1.1a can also be written as

$$\frac{dM}{dt} = rM, \quad (9.1.1b)$$

with r denoting the per-capita rate of cell division. The solution of this expression is

$$M(t) = M(0) \cdot e^{rt}, \quad (9.1.1c)$$

where

$$r = m_{AA} \cdot k_T \cdot f_R/m_R, \quad (9.1.2a)$$

which can be condensed to a simpler form

$$r = K_R \cdot f_R, \quad (9.1.2b)$$

with $K_R = m_{AA}k_T/m_R$ being a measure of the translational capacity of the system (the rate of protein mass produced per unit mass of extended ribosomes).

Although the preceding derivation assumes that all ribosomes are actively engaged in translation, if a subfraction $f_{R,0}$ is inactive (independent of growth conditions), then

$$r = K_R \cdot (f_R - f_{R,0}), \quad (9.1.2c)$$

which rearranges to

$$f_R = f_{R,0} + \left(\frac{r}{K_R} \right). \quad (9.1.3)$$

The central assumptions in the preceding derivations are that the translation rate of engaged ribosomes (k_T) and the fraction of unoccupied ribosomes ($f_{R,0}$) are invariant with respect to growth rate. Under such conditions and subject to the constraint that $f_R \leq 1$, Equation 9.1.3 predicts a linear relationship between the fraction of protein invested in extended ribosomes and the rate of cell division, with the intercept being equivalent to the fraction of total cellular protein associated with unengaged ribosomes, and the slope ($1/K_R$) measuring the inverse of the translational capacity. If $f_{R,0}$ and K_R are functions of r , the scaling relationship in Equation 9.1.3 would be altered.

Foundations 9.2. Nutrient limitation and cell growth. In Foundations 9.1, an expression was derived for the rate of cellular growth in terms of ribosome processing. An alternative expression for the growth rate can be couched in terms of the rate of conversion of a limiting nutrient into biomass, again represented by the total mass of protein M . Under steady-state conditions, both approaches must yield equivalent answers for the rate of cell growth, as the rate of amino-acid uptake/biosynthesis must equal the rate at which amino acids are incorporated into proteins at steady state.

We first introduce this second approach, and then unify the two into a joint expression. Again following Scott et al. (2010), we let

$$\frac{dM}{dt} = c \cdot k_E \cdot M_E, \quad (9.2.1a)$$

where c is a constant representing the conversion of the nutrient into M , and M_E is the summed mass of the proteins involved in nutrient acquisition and conversion into amino acids,

$$k_E = k_{E,\max} \left(\frac{S}{K_S + S} \right), \quad (9.2.1b)$$

is the rate of nutrient acquisition per mass of enzyme protein, following the Michaelis-Menten form, which depends on the nutrient concentration (S), and the half-saturation constant (K_S).

We now assume that the total protein in a cell (M) can be partitioned into three sectors (Figure 9.12): a fraction taken to be quantitatively (although not necessarily qualitatively) invariant with respect to cell physiology; a fraction consisting entirely of ribosomal proteins and other proteins associated with translation (extended ribosomes, as in Foundations 9.1); and a fraction associated with metabolic features that respond to nutritional changes. Letting these three fractions be f_Q , f_R , and f_P respectively, the system is constrained to obey

$$1 = f_Q + f_R + f_P. \quad (9.2.2)$$

Because f_Q is taken to be a constant, this means that increased investment in nutrient acquisition (f_P) necessitates a parallel reduction in investment in protein production (f_R), as the two must sum to $1 - f_Q$.

Further letting f_E denote the fraction of protein mass in sector P devoted to uptake of the limiting nutrient, i.e., $f_E = M_E/M_P$, and recalling from Foundations 9.1 that $f_P = M_P/M$, Equation 9.2.1a expands to

$$\frac{dM}{dt} = (c \cdot k_E \cdot f_E \cdot f_P) \cdot M. \quad (9.2.3)$$

As in Foundations 9.1, the product within the parentheses is equivalent to the rate of exponential growth, which can be further abbreviated to

$$r = K_N \cdot f_P, \quad (9.2.4)$$

where $K_N = c \cdot k_E \cdot f_E$ can be viewed as the nutritional capacity of the system.

We next wish to generate a more general growth-rate expression taking into joint consideration the underlying details about both translation (Foundations 9.1) and nutrient uptake. The key points are that under balanced growth: 1) the rate of nutrient conversion into biomass must be equivalent to the rate of protein production by ribosomes; and 2) the flexible fraction of the proteome must be apportioned into the fractions associated with translation (f_R) and nutrient provisioning (f_P).

As noted above, given that $f_R + f_P = 1 - f_Q$, there is an intrinsic tradeoff between the two processes. The maximum possible fractional allocation to ribosomes (or to the remaining pool) is $f_{R,\max} = (1 - f_Q)$, or in other words,

$$f_R = f_{R,\max} - f_P. \quad (9.2.5)$$

Recalling Equation 9.1.2c and substituting for f_R from the preceding expression,

$$r = K_R \cdot (f_{R,\max} - f_{R,0} - f_P), \quad (9.2.6)$$

where, as in Foundations 9.1, K_R is a measure of translational capacity, and $f_{R,0}$ is the fraction of investment in inactive ribosomes. Further substitution for f_P from Equation 9.2.4 and some rearrangement leads to the overall solution

$$r = K_R \cdot (f_{R,\max} - f_{R,0}) \cdot \left(\frac{K_N}{K_R + K_N} \right), \quad (9.2.7)$$

This expression provides a mechanistic link between nutrient uptake and conversion to protein biomass by ribosomes. In effect, it describes the situation in which the allocation to R and P proteins, f_R and f_P , is mutually adjusted such that the rate of intake of critical nutrients is matched by the rate of conversion into protein, subject to the constraint that these must sum to $1 - f_Q$. The fraction in large parentheses on the right is a function of the translation and nutritional capacities of the system, with the cell growth rate $r \rightarrow 0$ as $K_N \rightarrow 0$, and r asymptotically approaching a maximum value of $K_R \cdot (f_{R,\max} - f_{R,0})$ as $K_N \rightarrow \infty$. Because the fraction on the right equals 0.5 when $K_R = K_N$, the ribosomal capacity can be viewed as the half-saturation constant for nutrient capacity. Thus, despite the added complexities, the overall expression for r retains the form of a Monod growth equation.

This kind of partitioning model can be taken in a number of other interesting directions. For example, it has long been known that cells under chronically high nutrient levels often switch to seemingly inefficient modes of energy production, e.g., engagement in fermentation processes, which leave incompletely oxidized products such as acetate or lactate, as opposed to the citric acid cycle, which oxidizes glucose all the way down to CO_2 . Such metabolic overflow, or energy spillage, at high resource levels can be explained by the fact that the machinery underlying fermentation processes involves many fewer enzymes than that required for the citric acid cycle (Molenaar et al. 2009; Basan et al. 2015). The hypothesis here is that when the external carbon supply is high, cells can increase the investment in the protein machinery necessary for biosynthesis by reducing the investment in the enzymes necessary for input into such pathways. In contrast, when the nutrient supply is low, investing more heavily in carbon metabolism allows cells to maximally direct flux towards biosynthesis.

Bertaux et al. (2020) and Serbanescu et al. (2020) have extended the preceding model to incorporate additional sector partitioning, e.g., cell division. These extensions

allow for analysis of the size-growth rate relationship discussed in the text. There is room for caution in overinterpreting the good fits of models like these, as a large number of parameters are employed, not all of which are based on extrinsic estimates. The value of the approach resides in helping to highlight the potential importance of broad classes of underlying mechanisms that can be followed up by further empirical study. Extensive details on the underlying proteomic responses of *E. coli* cells to changing nutritional conditions are provided in synthetic reviews by Belliveau et al. (2021) and Mori et al. (2021).

Foundations 9.3. Scaling models for the development of cellular features.

Given what little we know about the mechanisms driving the quantitative relationships between cells and their parts during cell growth, consideration of alternative models may be informative, particularly if they predict different patterns of scaling.

Here, following Equation 9.7, we evaluate two fairly general models, in both cases assuming exponential growth of the cell at rate r in terms of total volume, i.e., $V_t = V_0 e^{rt}$. First, consider the situation in which a cellular feature grows exponentially and autonomously (i.e., independent of cell volume, V) at rate β , such that the expected phenotypic value at time t is

$$z_t = z_0 e^{\beta t}, \quad (9.3.1)$$

where z_0 is the phenotypic value at cell birth. Log transforming Equations 9.7 and 9.3.1, solving the first expression for t , and substituting into the latter, we obtain

$$\log(z_t) = \left(\frac{\beta}{r}\right) \log(V_t) + c, \quad (9.3.2a)$$

where

$$c = \log(z_0) - \left(\frac{\beta}{r}\right) \log(V_0), \quad (9.3.2b)$$

is the intercept of a log-log plot of z_t vs. V_t throughout developmental progression. Noting that c is a constant determined by the size of the trait and cell volume at birth (as well as the growth parameters β and r), this model predicts an allometric (power law; Chapter 8) relationship, with the slope providing an estimate of the ratio of growth rates (β/r). If the slope is equal to 1.0, then β must equal r , implying isometric growth.

Now consider the situation in which growth of the trait is directly linked to the growth in cell volume via some sort of regulatory mechanism (Harris and Theriot 2016), such that

$$\frac{dz}{dt} = \beta \cdot V_t = \beta \cdot V_0 e^{rt}, \quad (9.3.3)$$

the solution of which is

$$z_t = \left(\frac{\beta}{r}\right) V_t + c, \quad (9.3.4a)$$

with

$$c = z_0 - \left(\frac{\beta}{r}\right) V_0. \quad (9.3.4b)$$

Note that the key scaling parameter is again the ratio of growth rates, β/r . However, in contrast to the volume-independent model, where there is linear scaling between the log-transformed values of z_t and V_t , when trait growth is coupled directly to cell volume, the scaling is linear on the original scale of measurement. If $\beta \simeq r$, which the data in the text suggest for volumetric traits, these two models will be difficult to

distinguish based on growth-trajectory data alone. In both cases, the relationship will be essentially linear on the original scale of measurement.

Foundations 9.4. Parent-offspring resemblance and the response to selection. The measure of a particular trait in a specific individual, P , can be viewed as the sum of its expected value given its genotypic composition, G , and a deviation from that expectation, E , owing to both internal effects associated with stochastic molecular behavior and external effects associated with physical, chemical, and biological aspects of the environment,

$$P = G + E. \quad (9.4.1)$$

The genotypic value G can be thought of as the average phenotypic measure expected if a large number of individuals of the same genotype were monitored in an identical environmental setting. The environmental effect E summarizes the net positive or negative deviations around G , and has a mean (over all individuals) equal to zero and variance σ_E^2 among individuals (Lynch and Walsh 1998). Provided there is no genotype-environment covariance (i.e., environmental deviations are independent of the genetic background), the total phenotypic variance in the population is then the sum of the genetic and environmental variance components,

$$\sigma_P^2 = \sigma_G^2 + \sigma_E^2. \quad (9.4.2)$$

These variance components relate directly to the resemblance between relatives. If the offspring of measured parents are allowed to develop to the same stage as the parents and then measured, one can produce a parent-offspring regression, which is equivalent to the straight line that best describes the overall relationship (Figure 9.10). The slope of a best fit line is known to be equal to the ratio of the covariance between x and y variables (denoted as $\sigma(x, y)$, with the two variables here being offspring and parent phenotypes) and the variance of the x variable (denoted as $\sigma^2(x)$, and here applying to parental phenotypes). (For those unfamiliar with statistics, a variance is the average squared deviation of measures from the mean, whereas a covariance is the average cross-product of x and y deviations from their respective means). Letting o and p denote offspring and parents, and assuming asexual reproduction, the covariance between offspring and parent pairs expands to

$$\sigma(P_o, P_p) = \sigma[(G_o + E_o), (G_p + E_p)]. \quad (9.4.3a)$$

Although there are four potential cross-product terms in the covariance, assuming that the environmental deviations in different generations are uncorrelated (i.e., not inherited, an assumption relaxed in Foundations 9.5), there can only be covariance between the genetic values, so

$$\sigma(P_o, P_p) = \sigma(G_o, G_p), \quad (9.4.3b)$$

and because parents and offspring have identical genetic values in an asexual population, the genetic covariance is the same as the genetic variance,

$$\sigma(P_o, P_p) = \sigma_G^2. \quad (9.4.3c)$$

This follows because the covariance of a measure with itself is equal to the variance of the measure. The expected slope of the parent-offspring regression is then the ratio of Equations 9.4.3c and 9.4.2,

$$H^2 = \frac{\sigma_G^2}{\sigma_G^2 + \sigma_E^2}. \quad (9.4.4)$$

This quantity, which is usually referred to as the broad-sense heritability, is simply the fraction of the total phenotypic variance attributable to genetic causes. Further aspects concerning the phenotypic covariances among clonal relatives can be found in Jun et al. (2018). Slight modifications are required under sexual reproduction, as parents only transmit half their genetic value to their progeny (Lynch and Walsh 1998).

Foundations 9.5. Transient response to selection without genetic change.

Under the adder model for growth, Δ is equivalent to the expected increase in cell volume between cell divisions, and the expected size at birth is also Δ . This, however, is only strictly true in the absence of selection on cell size. Imagine a clonal population of cells with some variation in the realized value of Δ experienced by individual cells, owing to the vagaries in intracellular and external environments, and to the fact that cells do not divide with absolute symmetry.

With variation around the mean Δ , the size of an adult cell at the time of division can be expressed as

$$V_a = V_0 + \Delta + e_\Delta, \quad (9.5.1a)$$

where V_0 is the size at birth, Δ is the expected growth in size, and e_Δ is the deviation of the actual growth increment from Δ owing to background variation, assumed to have a mean value of zero and some variance σ_Δ^2 . In the absence of selection, the expected value of V_0 is Δ , and the previous expression can be written as

$$V_a = 2\Delta + \bar{e}_\Delta, \quad (9.5.1b)$$

with the expected offspring cell size being $\bar{V}_0 = \bar{V}_a/2 = \Delta$ because the expected value of e_Δ (denoted by the overline) is equal to zero.

If, however, there is directional selection on cell size, the mean value \bar{e}_Δ is no longer equal to zero, as the cells with more extreme deviations are differentially promoted. Instead, in the first generation of selection, the average offspring cell size becomes

$$\bar{V}_0(1) = \Delta + (\bar{e}_\Delta/2)$$

assuming that on average half of the mean environmental deviation in the previous generation is transmitted to each offspring cell. If this same level of selection is continued for another generation, the mean becomes

$$\bar{V}_0(2) = \Delta + (\bar{e}_\Delta/2) + (\bar{e}_\Delta/4)$$

as a new deviation is added while half of the prior deviation is partially removed by 50% dilution. Using the series expansion

$$\sum_{i=1}^t x^i = \frac{x(1-x^t)}{1-x}, \quad (9.5.2)$$

with $x = 0.5$, after t generations of constant selection, the mean offspring size is

$$\bar{V}_0(t) = \Delta + \bar{e}_\Delta [1 - (1/2)^t] \quad (9.5.3)$$

which asymptotically approaches $\Delta + \bar{e}_\Delta$ as t increases.

This shows that the average size of cells in a population can quickly shift to a new value without any genetic change, with a deviation from the nonselection value Δ equal to the selection differential \bar{e}_Δ . The central point is that owing to the partial

transmission of offspring deviations to subsequent generations, the mean phenotypes in a population are expected to change if directional selection persistently operates on a cellular trait, even if there is no genetic basis for the deviations.

Notably, however, this selection response is transient in that if selection is relaxed, the initial deviation \bar{e}_Δ declines by 50% each generation, rapidly returning offspring cell volume to Δ . In contrast, any genetic contribution to the selection response would remain following selection.

Finally, supposing extreme cells can sequester their excess endowment to a degree that allows greater than 50% retention, then the use of Equation 9.5.2 shows that an even greater transient boost can be obtained by selection on environmental deviations, e.g., with $x = 0.75$, $\bar{V}_0(t)$ has an asymptotic value of $\Delta + 3\bar{e}_\Delta$.

Literature Cited

- Ackermann, M. 2015. A functional perspective on phenotypic heterogeneity in microorganisms. *Nat. Rev. Microbiol.* 13: 497-508.
- Alberghina, F. A., E. Sturani, and J. R. Gohlke. 1975. Levels and rates of synthesis of ribosomal ribonucleic acid, transfer ribonucleic acid, and protein in *Neurospora crassa* in different steady states of growth. *J. Biol. Chem.* 250: 4381-4388.
- Amir, A. 2014. Cell size regulation in bacteria. *Phys. Rev. Lett.* 112: 208102.
- Amir A. 2017. Is cell size a spandrel? *eLife* 6: e22186.
- Atkinson, A. W., Jr., P. C. John, and B. E. Gunning. 1974. The growth and division of the single mitochondrion and other organelles during the cell cycle of *Chlorella*, studied by quantitative stereology and three dimensional reconstruction. *Protoplasma* 81: 77-109.
- Atkinson, D., B. J. Ciotti, and D. J. Montagnes. 2003. Protists decrease in size linearly with temperature: ca. 2.5% degrees C(-1). *Proc. Biol. Sci.* 270: 2605-2611.
- Baldwin, J. M. 1896. A new factor in evolution. *Amer. Natur.* 30: 441-451.
- Barenholz, U., L. Keren, E. Segal, and R. A. Milo. 2016. A minimalistic resource allocation model to explain ubiquitous increase in protein expression with growth rate. *PLoS One* 11: e0153344.
- Basan, M., S. Hui, H. Okano, Z. Zhang, Y. Shen, J. R. Williamson, and T. Hwa. 2015. Overflow metabolism in *Escherichia coli* results from efficient proteome allocation. *Nature* 528: 99-104.
- Belliveau, N. M., G. Chure, C. L. Hueschen, H. G. Garcia, J. Kondev, D. S. Fisher, J. A. Theriot, and R. Phillips. 2021. Fundamental limits on the rate of bacterial growth and their influence on proteomic composition. *Cell Syst.* 12: 924-944.e2.
- Bergeland, T., J. Widerberg, O. Bakke, and T. W. Nordeng. 2001. Mitotic partitioning of endosomes and lysosomes. *Curr. Biol.* 11: 644-651.
- Bergmann, K. G. L. C. 1847. Über die Verhältnisse der wärmeökonomie der Thiere zu ihrer Grösse. *Göttinger Studien* 3: 595-708.
- Bertaux, F., J. von Kügelgen, S. Marguerat, and V. Shahrezaei. 2020. A bacterial size law revealed by a coarse-grained model of cell physiology. *PLoS Comput. Biol.* 16: e1008245.
- Boehlke, K. W., and J. D. Friesen. 1975. Cellular content of ribonucleic acid and protein in *Saccharomyces cerevisiae* as a function of exponential growth rate: calculation of the apparent peptide chain elongation rate. *J. Bacteriol.* 121: 429-433.
- Bonven, B., and K. Gullov. 1979. Peptide chain elongation rate and ribosomal activity in *Saccharomyces cerevisiae* as a function of the growth rate. *Mol. Gen. Genet.* 170: 225-230.
- Brangwynne, C. P. 2013. Phase transitions and size scaling of membrane-less organelles. *J. Cell Biol.* 203: 875-881.
- Brown, C. M., and A. H. Rose. 1969. Effects of temperature on composition and cell volume of *Candida utilis*. *J. Bacteriol.* 97: 261-270.
- Bryan, A. K., A. Goranov, A. Amon, and S. R. Manalis. 2010. Measurement of mass, density, and volume during the cell cycle of yeast. *Proc. Natl. Acad. Sci. USA* 107: 999-1004.
- Bull, J. J. 1987. Evolution of phenotypic variance. *Evolution* 41: 303-315.

- Campos, M., I. V. Surovtsev, S. Kato, A. Paintdakhi, B. Beltran, S. E. Ebmeier, and C. Jacobs-Wagner. 2014. A constant size extension drives bacterial cell size homeostasis. *Cell* 159: 1433-1446.
- Cao, Z., and R. Grima. 2020. Analytical distributions for detailed models of stochastic gene expression in eukaryotic cells. *Proc. Natl. Acad. Sci. USA* 117: 4682-4692.
- Castellana, M., L. S. Hsin-Jung, and N. S. Wingreen. 2016. Spatial organization of bacterial transcription and translation. *Proc. Natl. Acad. Sci. USA* 113: 9286-9291.
- Chan, Y.-H., and W. F. Marshall. 2010. Scaling properties of cell and organelle size. *Organogenesis* 6: 88-96.
- Chan, Y.-H., and W. F. Marshall. 2012. How cells know the size of their organelles. *Science* 337: 1186-1189.
- Chan, Y.-H., and W. F. Marshall. 2014. Organelle size scaling of the budding yeast vacuole is tuned by membrane trafficking rates. *Biophys. J.* 106: 1986-1996.
- Chan, Y.-H., L. Reyes, S. M. Sohail, N. K. Tran, and W. F. Marshall. 2016. Organelle size scaling of the budding yeast vacuole by relative growth and inheritance. *Curr. Biol.* 26: 1221-1228.
- Chandler-Brown, D., K. M. Schmoller, Y. Winetraub, and J. M. Skotheim. 2017. The adder phenomenon emerges from independent control of pre- and post-start phases of the budding yeast cell cycle. *Curr. Biol.* 27: 2774-2783.
- Chien, A. C., S. K. Zareh, Y. M. Wang, and P. A. Levin. 2012. Changes in the oligomerization potential of the division inhibitor UgtP co-ordinate *Bacillus subtilis* cell size with nutrient availability. *Mol. Microbiol.* 86: 594-610.
- Colin, A., G. Micali, L. Faure, M. Cosentino Lagomarsino, and S. van Teeffelen. 2021. Two different cell-cycle processes determine the timing of cell division in *Escherichia coli*. *eLife* 10: e67495.
- das Neves, R. P., N. S. Jones, L. Andreu, R. Gupta, T. Enver, and F. J. Iborra. 2010. Connecting variability in global transcription rate to mitochondrial variability. *PLoS Biol.* 8: e1000560.
- Deforet, M., D. van Ditmarsch, and J. B. Xavier. 2015. Cell-size homeostasis and the incremental rule in a bacterial pathogen. *Biophys. J.* 109: 521-528.
- Delarue, M., D. Weissman, and O. Hallatschek. 2017. A simple molecular mechanism explains multiple patterns of cell-size regulation. *PLoS One* 12: e0182633.
- Dennis, P. P., and H. Bremer. 1974. Macromolecular composition during steady-state growth of *Escherichia coli* B-r. *J. Bacteriol.* 119: 270-281.
- Deviri, D., and S. A. Safran. 2022. Balance of osmotic pressures determines the nuclear-to-cytoplasmic volume ratio of the cell. *Proc. Natl. Acad. Sci. USA* 119: e2118301119.
- Di Talia, S., J. M. Skotheim, J. M. Bean, E. D. Siggia, and F. R. Cross. 2007. The effects of molecular noise and size control on variability in the budding yeast cell cycle. *Nature* 448: 947-951.
- Droop, M. R. 1973. Some thoughts on nutrient limitation in algae. *J. Phycol.* 9: 264-272.
- Droop, M. R. 1974. The nutrient status of algal cells in continuous culture. *J. Marine Biol. Assoc. United Kingdom* 54: 825-855.
- Droop, M. R. 1983. 25 years of algal growth kinetics: a personal view. *Botanica Marina* 26: 99-112.

- Eldar, A., and M. B. Elowitz. 2010. Functional roles for noise in genetic circuits. *Nature* 467: 167-173.
- Eun, Y. J., P. Y. Ho, M. Kim, S. LaRussa, L. Robert, L. D. Renner, A. Schmid, E. Garner, and A. Amir. 2018. Archaeal cells share common size control with bacteria despite noisier growth and division. *Nat. Microbiol.* 3: 148-154.
- Fantes, P. A. 1977. Control of cell size and cycle time in *Schizosaccharomyces pombe*. *J. Cell Sci.* 24: 51-67.
- Ferrezuelo, F., N. Colomina, A. Palmisano, E. Garí, C. Gallego, A. Csikász-Nagy, and M. Aldea. 2012. The critical size is set at a single-cell level by growth rate to attain homeostasis and adaptation. *Nat. Commun.* 3: 1012.
- Forchhammer, J., and L. Lindahl. 1971. Growth rate of polypeptide chains as a function of the cell growth rate in a mutant of *Escherichia coli*. *J. Mol. Biol.* 55: 563-568.
- Fraenkel, D. G., and F. C. Neidhardt. 1961. Use of chloramphenicol to study control of RNA synthesis in bacteria. *Biochim. Biophys. Acta* 53: 96-110.
- Fraser, D., and M. Kaern. 2009. A chance at survival: gene expression noise and phenotypic diversification strategies. *Mol. Microbiol.* 71: 1333-1340.
- Freyssinet, G., and J. A. Schiff. 1974. The chloroplast and cytoplasmic ribosomes of *Euglena*: II. Characterization of ribosomal proteins. *Plant Physiol.* 53: 543-554.
- Froese, G. 1964. The distribution and interdependence of generation times of HeLa cells. *Exp. Cell Res.* 35: 415-419.
- Fu, R., and J. Gong. 2017. Single cell analysis linking ribosomal (r)DNA and rRNA copy numbers to cell size and growth rate provides insights into molecular protistan ecology. *J. Eukaryot. Microbiol.* 64: 885-896.
- Geiler-Samerotte, K. A., C. R. Bauer, S. Li, N. Ziv, D. Gresham, and M. L. Siegal. 2013. The details in the distributions: why and how to study phenotypic variability. *Curr. Opin. Biotechnol.* 24: 752-759.
- Godin, M., F. F. Delgado, S. Son, W. H. Grover, A. K. Bryan, A. Tzur, P. Jorgensen, K. Payer, A. D. Grossman, M. W. Kirschner, et al. 2010. Using buoyant mass to measure the growth of single cells. *Nat. Methods* 7: 387-390.
- Goehring, N. W., and A. A. Hyman. 2012. Organelle growth control through limiting pools of cytoplasmic components. *Curr. Biol.* 22: R330-R339.
- Gray, W. T., S. K. Govers, Y. Xiang, B. R. Parry, M. Campos, S. Kim, and C. Jacobs-Wagner. 2019. Nucleoid size scaling and intracellular organization of translation across bacteria. *Cell* 177: 1632-1648.
- Harris, L. K., and J. A. Theriot. 2016. Relative rates of surface and volume synthesis set bacterial cell size. *Cell* 165: 1479-1492.
- Harvey, R. J., A. G. Marr, and P. R. Painter. 1967. Kinetics of growth of individual cells of *Escherichia coli* and *Azotobacter agilis*. *J. Bacteriol.* 93: 605-617.
- Hashimoto, M., T. Nozoe, H. Nakaoka, R. Okura, S. Akiyoshi, K. Kaneko, E. Kussell, and Y. Wakamoto. 2016. Noise-driven growth rate gain in clonal cellular populations. *Proc. Natl. Acad. Sci. USA* 113: 3251-3256.

- Homma, K., and J. W. Hastings. 1989. Cell growth kinetics, division asymmetry and volume control at division in the marine dinoflagellate *Gonyaulax polyedra*: a model of circadian clock control of the cell cycle. *J. Cell Sci.* 92: 303-318.
- Huh, D., and J. Paulsson. 2011. Random partitioning of molecules at cell division. *Proc. Natl. Acad. Sci. USA* 108: 15004-15009.
- Iyer-Biswas, S., C. S. Wright, J. T. Henry, K. Lo, S. Burov, Y. Lin, G. E. Crooks, S. Crosson, A. R. Dinner, and N. F. Scherer. 2014. Scaling laws governing stochastic growth and division of single bacterial cells. *Proc. Natl. Acad. Sci. USA* 111: 15912-15917.
- Jacob, F. 1998. *The Statue Within: an Autobiography*. Cold Spring Harbor Laboratory Press, Cold Spring Harbor, NY.
- Jahn, M., S. Günther, and S. Müller. 2015. Non-random distribution of macromolecules as driving forces for phenotypic variation. *Curr. Opin. Microbiol.* 25: 49-55.
- Jajoo, R., Y. Jung, D. Huh, M. P. Viana, S. M. Rafelski, M. Springer, and J. Paulsson. 2016. Accurate concentration control of mitochondria and nucleoids. *Science* 351: 169-172.
- Johnson, B. F., G. B. Calleja, I. Boisclair, and B. Y. Yoo. 1979. Cell division in yeasts. III. The biased, asymmetric location of the septum in the fission yeast cell, *Schizosaccharomyces pombe*. *Exp. Cell Res.* 123: 253-259.
- Johnston, I. G., B. Gaal, R. P. Neves, T. Enver, F. J. Iborra, and N. S. Jones. 2012. Mitochondrial variability as a source of extrinsic cellular noise. *PLoS Comput. Biol.* 8: e1002416.
- Jorgensen, P., N. P. Edgington, B. L. Schneider, I. Rupes, M. Tyers, and B. Futcher. 2007. The size of the nucleus increases as yeast cells grow. *Mol. Biol. Cell* 18: 3523-3532.
- Jun, S., F. Si, R. Pugatch, and M. Scott. 2018. Fundamental principles in bacterial physiology-history, recent progress, and the future with focus on cell size control: a review. *Rep. Prog. Phys.* 81: 056601.
- Kendall, D. G. 1948. On the role of variable generation time in the development of a stochastic birth process. *Biometrika* 35: 316-330.
- Keren, L., D. van Dijk, S. Weingarten-Gabbay, D. Davidi, G. Jona, A. Weinberger, R. Milo, and E. Segal. 2015. Noise in gene expression is coupled to growth rate. *Genome Res.* 25: 1893-1902.
- Kimball, R. F., T. O. Casperson, G. Svensson, and L. Carlson. 1959. Quantitative cytochemical studies on *Paramecium aurelia*. I. Growth in total dry weight measured by the scanning interference microscope and x-ray absorption methods. *Exp. Cell. Res.* 17: 160-172.
- Kiviet, D. J., P. Nghe, N. Walker, S. Boulineau, V. Sunderlikova, and S. J. Tans. 2014. Stochasticity of metabolism and growth at the single-cell level. *Nature* 514: 376-379.
- Koch, A. L., and M. Schaechter. 1962. A model for statistics of the cell division process. *J. Gen. Microbiol.* 29: 435-454.
- Krásný, L., and R. L. Gourse. 2004. An alternative strategy for bacterial ribosome synthesis: *Bacillus subtilis* rRNA transcription regulation. *EMBO J.* 23: 4473-4483.
- Kuchen, E. E., N. B. Becker, N. Claudino, and T. Höfer. 2020. Hidden long-range memories of growth and cycle speed correlate cell cycles in lineage trees. *eLife* 9: e51002.
- Kussell, E., and S. Leibler. 2005. Phenotypic diversity, population growth, and information in

- fluctuating environments. *Science* 309: 2075-2078.
- Lemière, J., P. Real-Calderon, L. J. Holt, T. G. Fai, and F. Chang. 2022. Control of nuclear size by osmotic forces in *Schizosaccharomyces pombe*. *eLife* 11: e76075.
- Lenski, R. E., and M. Travisano. 1994. Dynamics of adaptation and diversification: a 10,000-generation experiment with bacterial populations. *Proc. Natl. Acad. Sci. USA* 91: 6808-6814.
- Levy, D. L., and R. Heald. 2012. Mechanisms of intracellular scaling. *Annu. Rev. Cell Dev. Biol.* 28: 113-135.
- Levy, S. F., N. Ziv, and M. L. Siegal. 2012. Bet hedging in yeast by heterogeneous, age-correlated expression of a stress protectant. *PLoS Biol.* 10: e1001325.
- Litsios, A., D. H. E. W. Huberts, H. M. Terpstra, P. Guerra, A. Schmidt, K. Buczak, A. Papiannakis, M. Rovetta, J. Hekelaar, G. Hubmann, et al. 2019. Differential scaling between G1 protein production and cell size dynamics promotes commitment to the cell division cycle in budding yeast. *Nat. Cell Biol.* 21: 1382-1392.
- Liu, K., A. N. Bittner, and J. D. Wang. 2015. Diversity in (p)ppGpp metabolism and effectors. *Curr. Opin. Microbiol.* 24: 72-79.
- Logsdon, M. M., P. Y. Ho, K. Papavinasasundaram, K. Richardson, M. Cokol, C. M. Sassetti, A. Amir, and B. B. Aldridge. 2017. A parallel adder coordinates mycobacterial cell-cycle progression and cell-size homeostasis in the context of asymmetric growth and organization. *Curr. Biol.* 27: 3367-3374.
- Losick, R., and C. Desplan. 2008. Stochasticity and cell fate. *Science* 320: 65-68.
- Lutkenhaus, J. 2008. Min oscillation in bacteria. *Adv. Exp. Med. Biol.* 641: 49-61.
- Lynch, M., and J. B. Walsh. 1998. *Genetics and Analysis of Quantitative Traits*. Sinauer Assoc., Inc., Sunderland, MA.
- Maitra, A., and K. A. Dill. 2015. Bacterial growth laws reflect the evolutionary importance of energy efficiency. *Proc. Natl. Acad. Sci. USA* 112: 406-411.
- McInally, S. G., J. Kondev, and B. L. Goode. 2021. Scaling of subcellular actin structures with cell length through decelerated growth. *eLife* 10: e68424.
- Metzl-Raz, E., M. Kafri, G. Yaakov, I. Soifer, Y. Gurvich, and N. Barkai. 2017. Principles of cellular resource allocation revealed by condition-dependent proteome profiling. *eLife* 6: e28034.
- Mir, M., Z. Wang, Z. Shen, M. Bednarz, R. Bashir, I. Golding, S. G. Prasanth, and G. Popescu. 2011. Optical measurement of cycle-dependent cell growth. *Proc. Natl. Acad. Sci. USA* 108: 13124-13129.
- Mochizuki, T. 1998. Three-dimensional reconstruction of mitotic cells of *Cryptococcus neoformans* based on serial section electron microscopy. *Nihon Ishinkin Gakkai Zasshi* 39: 123-127.
- Molenaar, D., R. van Berlo, D. de Ridder, and B. Teusink. 2009. Shifts in growth strategies reflect tradeoffs in cellular economics. *Mol. Syst. Biol.* 5: 323.
- Monod, J. 1949. The growth of bacterial cultures. *Ann. Rev. Microbiol.* 3: 371-394.
- Mori, M., S. Schink, D. W. Erickson, U. Gerland, and T. Hwa. 2017. Quantifying the benefit of a proteome reserve in fluctuating environments. *Nat. Commun.* 8: 1225.

- Mori, M., Z. Zhang, A. Banaei-Esfahani, J. B. Lallane, H. Okano, B. C. Collins, A. Schmidt, O. T. Schubert, D. S. Lee, G. W. Li, et al. 2021. From coarse to fine: the absolute *Escherichia coli* proteome under diverse growth conditions. *Mol. Syst. Biol.* 17: e9536.
- Moseley, J. B., A. Mayeux, A. Paoletti, and P. Nurse. 2009. A spatial gradient coordinates cell size and mitotic entry in fission yeast. *Nature* 459: 857-860.
- Nanninga, N., L. J. Koppes, and F. C. de Vries-Tijssen. 1979. The cell cycle of *Bacillus subtilis* as studied by electron microscopy. *Arch. Microbiol.* 123: 173-181.
- Neumann, F. R., and P. Nurse. 2007. Nuclear size control in fission yeast. *J. Cell Biol.* 179: 593-600.
- Osella, M., E. Nugent, and M. Cosentino Lagomarsino. 2014. Concerted control of *Escherichia coli* cell division. *Proc. Natl. Acad. Sci. USA* 111: 3431-3435.
- Parenteau, J., L. Maignon, M. Berthoumieux, M. Catala, V. Gagnon, and S. Abou Elela. 2019. Introns are mediators of cell response to starvation. *Nature* 565: 612-617.
- Pearl Mizrahi, S., O. Sandler, L. Lande-Diner, N. Q. Balaban, and I. Simon. 2016. Distinguishing between stochasticity and determinism: examples from cell cycle duration variability. *Bioessays* 38: 8-13.
- Pellegrini, M. 1980. Three-dimensional reconstruction of organelles in *Euglena gracilis* Z. II. Qualitative and quantitative changes of chloroplasts and mitochondrial reticulum in synchronous cultures during bleaching. *J. Cell Sci.* 46: 313-340.
- Plaut, B. S., and G. Turnock. 1975. Coordination of macromolecular synthesis in the slime mould *Physarum polycephalum*. *Mol. Gen. Genet.* 137: 211-225.
- Posakony, J. W., J. M. England, and G. Attardi. 1977. Mitochondrial growth and division during the cell cycle in HeLa cells. *J. Cell Biol.* 74: 468-491.
- Potrykus, K., H. Murphy, N. Philippe, and M. Cashel. 2011. ppGpp is the major source of growth rate control in *E. coli*. *Environ. Microbiol.* 13: 563-575.
- Powell, E. O. 1956. Growth rate and generation time of bacteria, with special reference to continuous culture. *J. Gen. Microbiol.* 15: 492-511.
- Powell, E. O. 1958. An outline of the pattern of bacterial generation times. *J. Gen. Microbiol.* 18: 382-417.
- Poyton, R. O. 1973. Effect of growth rate on the macromolecular composition of *Prototheca zopfii*, a colorless alga which divides by multiple fission. *J. Bacteriol.* 113: 203-211.
- Priestman, M., P. Thomas, B. D. Robertson, and V. Shahrezaei. 2017. Mycobacteria modify their cell size control under sub-optimal carbon sources. *Front. Cell Dev. Biol.* 5: 64.
- Prokop, A., and J. Ríca. 1968. *Chlorella pyrenoidosa* 7-11-05 in batch and in homogeneous continuous culture under autotrophic conditions. I. Growth characteristics of the culture. *Folia Microbiol (Praha)* 13: 353-361.
- Rafelski, S. M., M. P. Viana, Y. Zhang, Y.-H. Chan, K. S. Thorn, P. Yam, J. C. Fung, H. Li, F. Costa Lda, and W. F. Marshall. 2012. Mitochondrial network size scaling in budding yeast. *Science* 338: 822-824.
- Rhee, A., R. Cheong, and A. Levchenko. 2014. Noise decomposition of intracellular biochemical

- signaling networks using nonequivalent reporters. *Proc. Natl. Acad. Sci. USA* 111: 17330-17335.
- Riemer, K., R. P. Guralnick, and E. P. White. 2018. No general relationship between mass and temperature in endothermic species. *eLife* 7: e27166.
- Rosset, R., R. Monier, and J. Julien. 1964. RNA composition of *Escherichia coli* as a function of growth rate. *Biochem. Biophys. Res. Comm.* 15: 329-333.
- Sandler, O., S. P. Mizrahi, N. Weiss, O. Agam, I. Simon, and N. Q. Balaban. 2015. Lineage correlations of single cell division time as a probe of cell-cycle dynamics. *Nature* 519: 468-471.
- Santi, I., N. Dhar, D. Bousbaine, Y. Wakamoto, and J. D. McKinney. 2013. Single-cell dynamics of the chromosome replication and cell division cycles in mycobacteria. *Nat. Commun.* 4: 2470.
- Schaechter, M., O. Maaløe, and N. O. Kjeldgaard. 1958. Dependency on medium and temperature of cell size and chemical composition during balanced grown of *Salmonella typhimurium*. *J. Gen. Microbiol.* 19: 592-606.
- Schaechter, M., J. P. Williamson, J. R. Hood, Jr., and A. L. Koch. 1962. Growth, cell and nuclear divisions in some bacteria. *J. Gen. Microbiol.* 29: 421-434.
- Scherbaum, O., and G. Rasch. 1957. Cell size distribution and single cell growth in *Tetrahymena pyriformis* G11. *Acta Pathol. Microbiol.* 41: 161-182.
- Schmoller, K. M., J. J. Turner, M. Kõivomägi, and J. M. Skotheim. 2015. Dilution of the cell cycle inhibitor Whi5 controls budding-yeast cell size. *Nature* 526: 268-272.
- Scott, M., C. W. Gunderson, E. M. Mateescu, Z. Zhang, and T. Hwa. 2010. Interdependence of cell growth and gene expression: origins and consequences. *Science* 330: 1099-1102.
- Serbanescu, D., N. Ojkic, and S. Banerjee. 2020. Nutrient-dependent trade-offs between ribosomes and division protein synthesis control bacterial cell size and growth. *Cell Rep.* 32: 108183.
- Si, F., G. Le Treut, J. T. Sauls, S. Vadia, P. A. Levin, and S. Jun. 2019. Mechanistic origin of cell-size control and homeostasis in bacteria. *Curr. Biol.* 29: 1760-1770.
- Si, F., D. Li, S. E. Cox, J. T. Sauls, O. Azizi, C. Sou, A. B. Schwartz, M. J. Erickstad, Y. Jun, X. Li, et al. 2017. Invariance of initiation mass and predictability of cell size in *Escherichia coli*. *Curr. Biol.* 27: 1278-1287.
- Soifer, I., and N. Barkai. 2014. Systematic identification of cell size regulators in budding yeast. *Mol. Syst. Biol.* 10: 761.
- Soifer, I., L. Robert, and A. Amir. 2016. Single-cell analysis of growth in budding yeast and bacteria reveals a common size regulation strategy. *Curr. Biol.* 26: 356-361.
- Sompayrac, L., and O. Maaløe. 1973. Autorepressor model for control of DNA replication. *Nat. New Biol.* 241: 133-135.
- Staudte, R. G., J. Zhang, R. M. Huggins, and R. Cowan. 1996. A reexamination of the cell-lineage data of E. O. Powell. *Biometrics* 52: 1214-1222.
- Susman, L., M. Kohram, H. Vashistha, J. T. Nechleba, H. Salman, and N. Brenner. 2018. Individuality and slow dynamics in bacterial growth homeostasis. *Proc. Natl. Acad. Sci. USA* 115: E5679-E5687.
- Sveiczzer, A., B. Novak, and J. M. Mitchison. 1996. The size control of fission yeast revisited. *J. Cell Sci.* 109: 2947-2957.

- Taheri-Araghi, S., S. Bradde, J. T. Sauls, N. S. Hill, P. A. Levin, J. Paulsson, M. Vergassola, and S. Jun. 2015. Cell-size control and homeostasis in bacteria. *Curr. Biol.* 25: 385-391.
- Tanaka, K., T. Kanbe, and T. Kuroiwa. 1985. Three-dimensional behaviour of mitochondria during cell division and germ tube formation in the dimorphic yeast *Candida albicans*. *J. Cell Sci.* 73: 207-220.
- Tanouchi, Y., A. Pai, H. Park, S. Huang, R. Stamatov, N. E. Buchler, and L. You. 2015. A noisy linear map underlies oscillations in cell size and gene expression in bacteria. *Nature* 523: 357-360.
- Tempest, D. W., J. R. Hunter, and J. Sykes. 1965. Magnesium-limited growth of *Aerobacter aerogenes* in a chemostat. *J. Gen. Microbiol.* 39: 355-366.
- Thattai, M., and A. van Oudenaarden. 2004. Stochastic gene expression in fluctuating environments. *Genetics* 167: 523-530.
- Thompson, D. A. 1917. *On Growth and Form*. Cambridge Univ. Press, Cambridge, UK.
- Trueba, F. J. 1982. On the precision and accuracy achieved by *Escherichia coli* cells at fission about their middle. *Arch. Microbiol.* 131: 55-59.
- Turner, J. J., J. C. Ewald, and J. M. Skotheim. 2012. Cell size control in yeast. *Curr. Biol.* 22: R350-R359.
- Tyson, J. J. 1989. Effects of asymmetric division on a stochastic model of the cell division cycle. *Math. Biosci.* 96: 165-184.
- Tyson, J. J., and K. B. Hannsgen. 1985. The distributions of cell size and generation time in a model of the cell cycle incorporating size control and random transitions. *J. Theor. Biol.* 113: 29-62.
- Tyson, J. J., and K. B. Hannsgen. 1985. Global asymptotic stability of the size distribution in probabilistic models of the cell cycle. *J. Math. Biol.* 22:61-68.
- Tyson, C. B., P. G. Lord, and A. E. Wheals. 1979. Dependency of size of *Saccharomyces cerevisiae* cells on growth rate. *J. Bacteriol.* 138: 92-98.
- Vallania, F. L., M. Sherman, Z. Goodwin, I. Mogno, B. A. Cohen, and R. D. Mitra. 2014. Origin and consequences of the relationship between protein mean and variance. *PLoS One* 9: e102202.
- Vashistha, H., M. Kohram, and H. Salman. 2021. Non-genetic inheritance restraint of cell-to-cell variation. *eLife* 10: e64779.
- Vila-Sanjurjo, A. 2008. Modification of the ribosome and the translational machinery during reduced growth due to environmental stress. *EcoSal Plus* 3(1).
- Volkmer, B., and M. Heinemann. 2011. Condition-dependent cell volume and concentration of *Escherichia coli* to facilitate data conversion for systems biology modeling. *PLoS One* 6: e23126.
- Voorn, W. J., and L. J. Koppes. 1998. Skew or third moment of bacterial generation times. *Arch. Microbiol.* 169: 43-51.
- Waddington, C. 1942. Canalization of development and the inheritance of acquired characters. *Nature* 150: 563-565.
- Waldron, C., and F. Lacroute. 1975. Effect of growth rate on the amounts of ribosomal and transfer ribonucleic acids in yeast. *J. Bacteriol.* 122: 855-865.

- Wallden, M., D. Fange, E. G. Lundius, Ö. Baltekin, and J. Elf. 2016. The synchronization of replication and division cycles in individual *E. coli* cells. *Cell* 166: 729-739.
- Warner, J. R., J. Vilardell, and J. H. Sohn. 2001. Economics of ribosome biosynthesis. *Cold Spring Harb. Symp. Quant. Biol.* 66: 567-574.
- Weart, R. B., A. H. Lee, A. C. Chien, D. P. Haeusser, N. S. Hill, and P. A. Levin. 2007. A metabolic sensor governing cell size in bacteria. *Cell* 130: 335-347.
- Weiß, A. Y., D. A. Oyarzún, V. Danos, and P. S. Swain. 2015. Mechanistic links between cellular trade-offs, gene expression, and growth. *Proc. Natl. Acad. Sci. USA* 112: E1038-E1047.
- Wolf, D. M., V. V. Vazirani, and A. P. Arkin. 2005. Diversity in times of adversity: probabilistic strategies in microbial survival games. *J. Theor. Biol.* 234: 227-253.
- Wu, C., R. Balakrishnan, N. Braniff, M. Mori, G. Manzanarez, Z. Zhang, and T. Hwa. 2022. Cellular perception of growth rate and the mechanistic origin of bacterial growth law. *Proc. Natl. Acad. Sci. USA* 119: e2201585119.
- Yoshida, H., and A. Wada. 2014. The 100S ribosome: ribosomal hibernation induced by stress. *Wiley Interdiscip. Rev. RNA* 5: 723-732.
- Yoshida, M., S. Tsuru, N. Hirata, S. Seno, H. Matsuda, B. W. Ying, and T. Yomo. 2014. Directed evolution of cell size in *Escherichia coli*. *BMC Evol. Biol.* 14: 257.
- Young, R., and H. Bremer. 1976. Polypeptide-chain-elongation rate in *Escherichia coli* B/r as a function of growth rate. *Biochem. J.* 160: 185-194.
- Yule, G. U. 1925. Mathematical theory of evolution, based on the conclusions of Dr. J. C. Willis, F.R.S. *Phil. Trans. Royal Soc. London Series B* 213: 21-87.
- Zalkinder, V. 1979. Correlation between cell nutrition, cell size and division control. Part I. *Biosystems* 11: 295-307.
- Zavřel, T., M. Faizi, C. Loureiro, G. Poschmann, K. Stühler, M. Sinetova, A. Zorina, R. Steuer, and J. Červený. 2019. Quantitative insights into the cyanobacterial cell economy. *eLife* 8: e42508.
- Zheng, H., Y. Bai, M. Jiang, T. A. Tokuyasu, X. Huang, F. Zhong, Y. Wu, X. Fu, N. Kleckner, T. Hwa, and C. Liu. 2020. General quantitative relations linking cell growth and the cell cycle in *Escherichia coli*. *Nat. Microbiol.* 5: 995-1001.
- Zhu, M., X. Dai, and Y. P. Wang. 2016. Real time determination of bacterial *in vivo* ribosome translation elongation speed based on LacZ α complementation system. *Nucleic Acids Res.* 44: e155.
- Zhuravel, D., D. Fraser, S. St.-Pierre, L. Tepliakova, W. L. Pang, J. Hasty, and M. Kaern. 2010. Phenotypic impact of regulatory noise in cellular stress-response pathways. *Syst. Synth. Biol.* 4: 105-116.
- Zohary, T., G. Flaim, and U. Sommer. 2021. Temperature and the size of freshwater phytoplankton. *Hydrobiol.* 848: 143-155.

Figure 9.1. Response of various cellular features associated with mRNA translation to changes in cellular growth rate. References: *Candida utilis* (Brown and Rose 1969); *Euglena gracilis* (Freysinet and Schiff 1974); *Neurospora crassa* (Alberghina et al. 1975); *Physarum polycephalum* (Plaut and Turnock 1975); *Prototheca zopfii* (Poyton 1973); *Saccharomyces cerevisiae* (Boehlke and Friesen 1975; Waldron and Lacroute 1975; Bonven and Gullov 1979; Metzl-Raz et al. 2017); *Escherichia coli* (Rosset et al. 1964; Forchhammer and Lindahl 1971; Dennis and Bremer 1974; Young and Bremer 1976; Scott et al. 2010; Zhu et al. 2016); *Aerobacter aerogenes* (Fraenkel and Neidhardt 1961; Tempest et al. 1965).

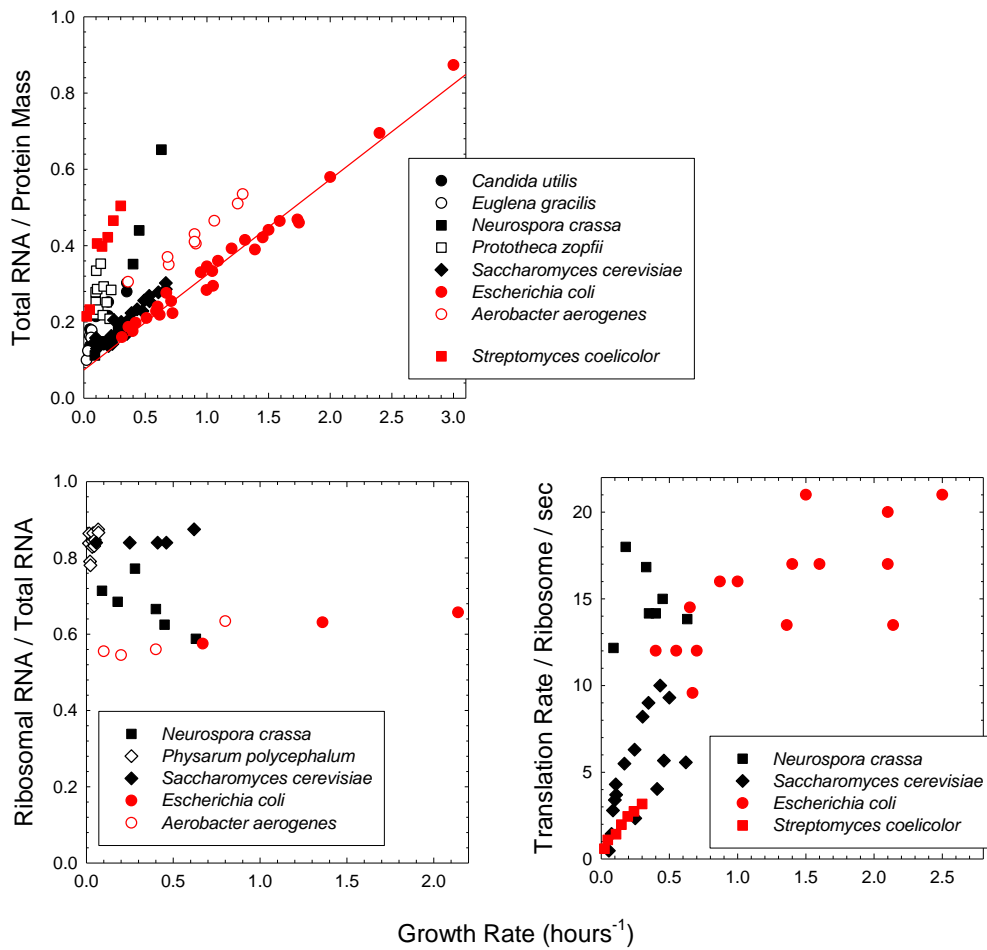


Figure 9.2. Various growth (r) and nutrient uptake (u) responses of the marine planktonic chryso-phyte alga *Monochrysis lutheri* to various concentrations of vitamin B₁₂, recorded for populations of cells grown in a chemostat. The upper left and right graphs provide the relationships between the cell-division rate and external and internal nutrient concentrations. The lower-right graph illustrates the inverse linear relationship between r and $1/Q$, as predicted by Equation 9.5. For the lower left panel, the straight-line relationship for the rate of nutrient uptake is derived from Equation 9.4b, which rearranges to $(1/u) = (1/u_{\max}) + (K_u/u_{\max})(1/S)$. The data are from Droop (1973, 1974, 1984).

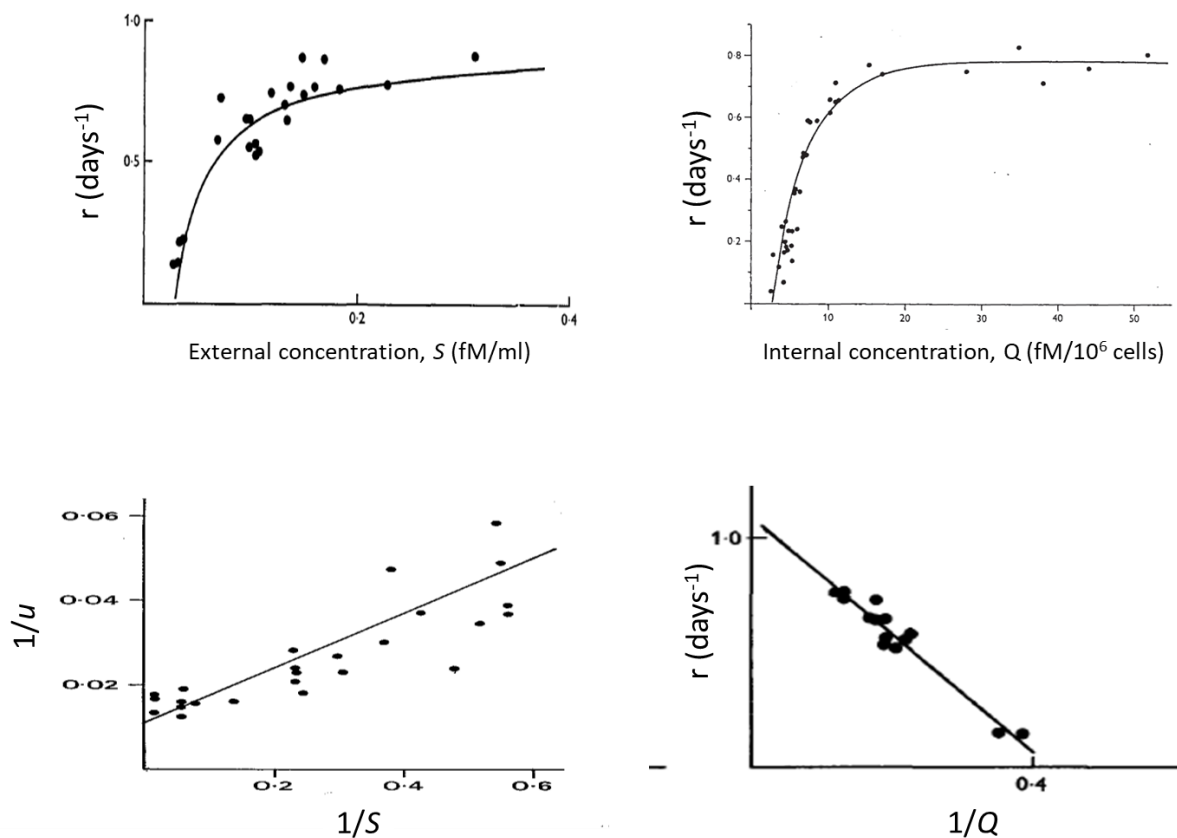


Figure 9.3. Expected relationship between cell volume at birth and at subsequent cell division under three alternative growth models. Δ serves as a reference point. Under the sizer model, regardless of the size at birth, the size at division always returns to 2Δ . Under the simplest form of the timer model, because of exponential growth, all cells grow by the same factor over a given duration, so individuals of extreme size produce offspring that are just as extreme; if there are stochastic deviations in offspring size or growth rates, the size distribution will diverge. Under the adder model, cells above or below the average still produce deviant progeny, but the average size of the progeny is less extreme than that of the parental cells, resulting in convergence of the cell-size distribution to an equilibrium.

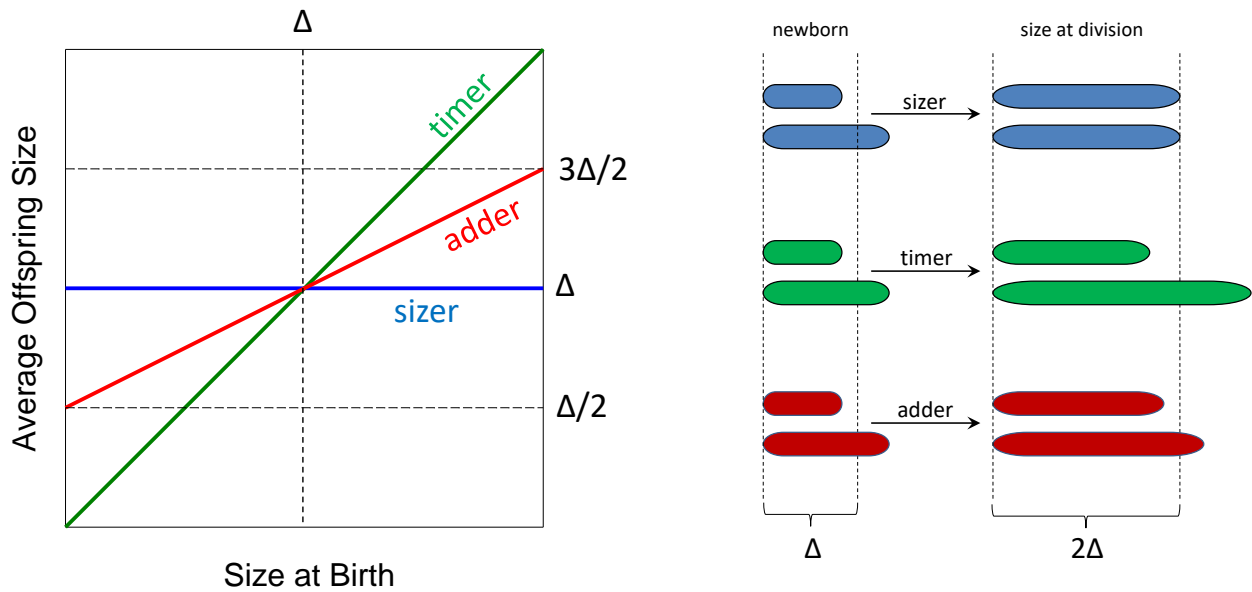


Figure 9.4. Evidence in support of the adder model for *E. coli* grown in different media. Proceeding from left to right, the growth media are increasingly rich sources of energy, carbon, and other nutrients. **Upper panel)** By looking at individual cells within each medium (at a constant concentration), it can be seen that the growth increments to maturity (Δ) are nearly independent of the size at birth. **Lower panel)** The inverse relationship between the cell-division time and cell volume at birth becomes progressively stronger in media that support lower growth rates. In the upper and lower panels, respectively, size is presented as cell length and cell volume, although the two are directly proportional, given that *E. coli* cells are nearly cylindrical in shape. Note that the adder model only provides a first-order approximation, as cells at the extremes of the size range deviate from expectations (upper panel). From Taheri-Araghi et al. (2015).

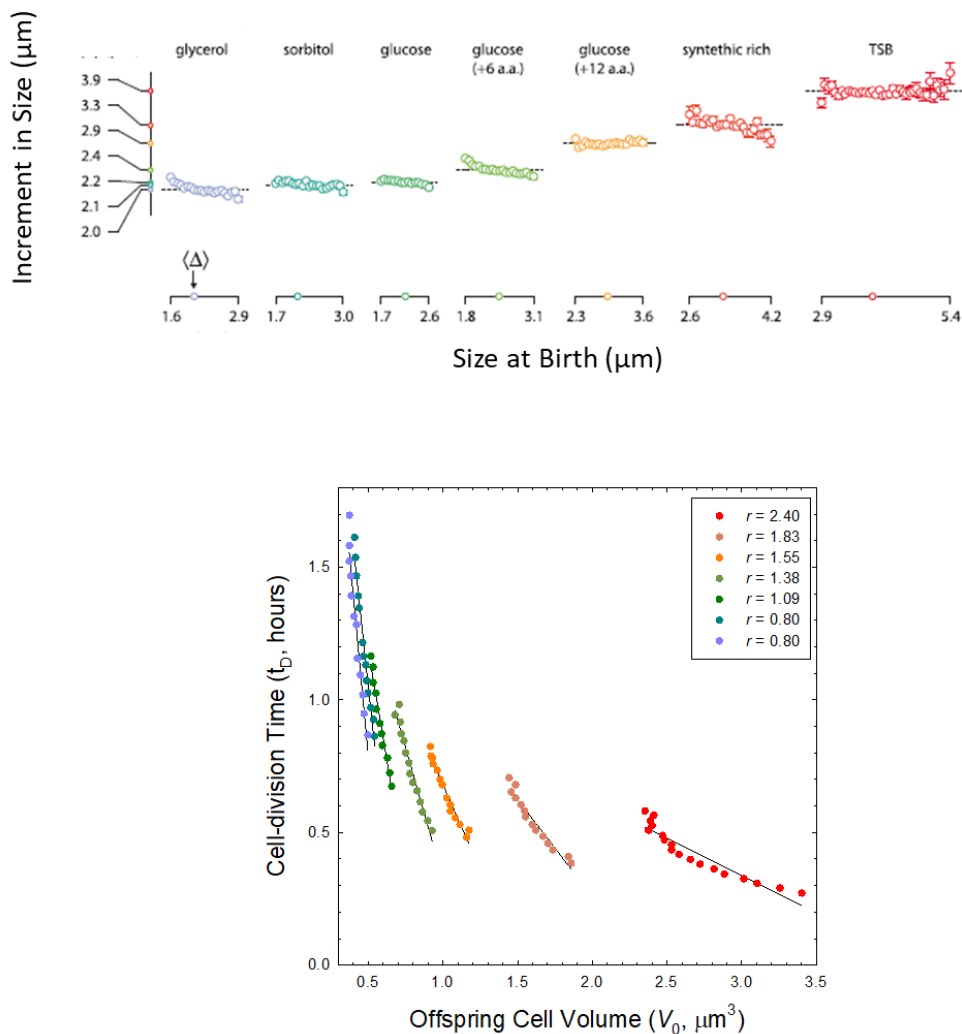


Figure 9.5. Two alternative models for the determination of cell size at division, presented in a generic fashion. On the left, a pulse of an inhibitor produced at the time of cell division experiences a progressive reduction in concentration as cell volume increases during growth; division occurs once the inhibitor concentration declines to a threshold level. On the right, an activator is continuously produced during cell growth, increasing in concentration until a critical level signals the time to division.

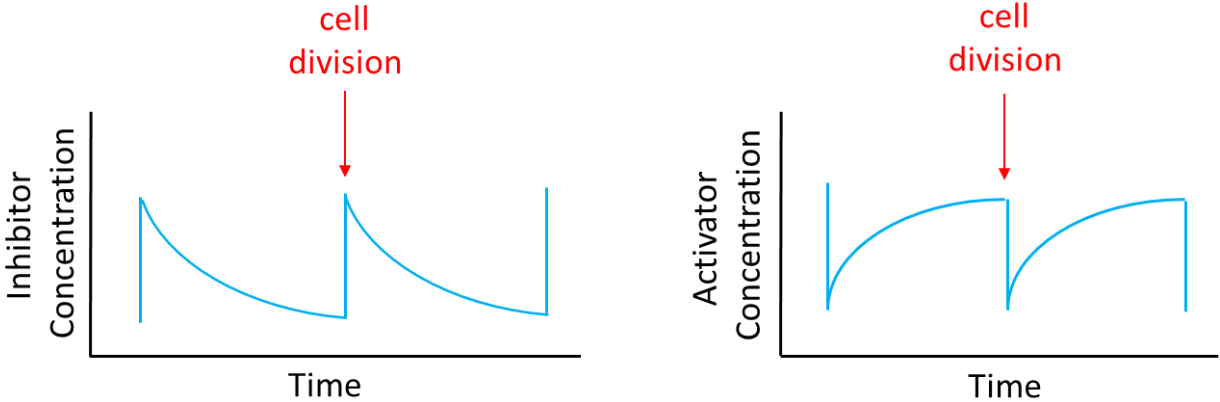


Figure 9.6. Evolutionary trajectories of cell-division rates and cell volume in a 10,000 generation experiment in which *E. coli* was subjected to persistent selection for higher growth rate. From Lenski and Travisano (1994).

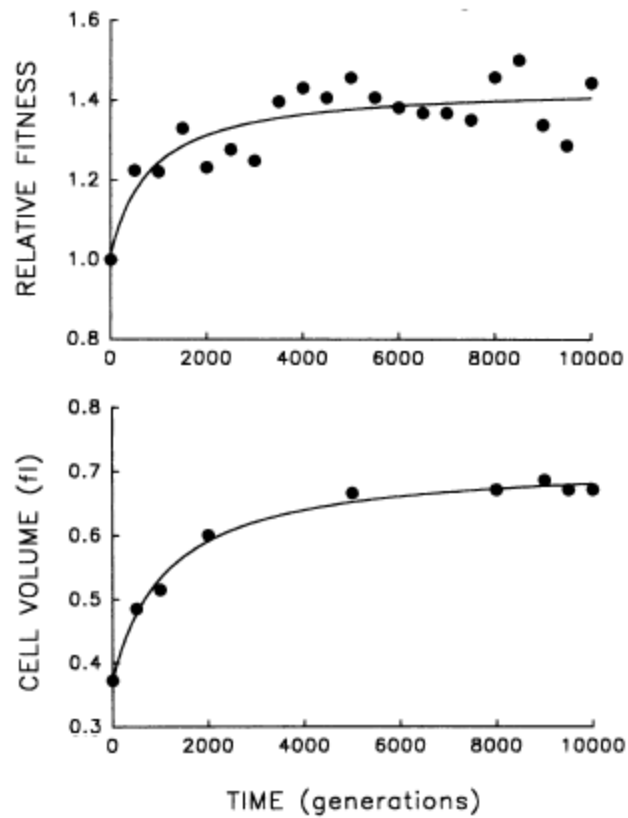


Figure 9.7. Idealized views of the response of cell growth rates to environmental effects. **A)** The solid black lines denote the phylogenetic relationship between the maximum rate of cellular growth, r_{\max} , taken from Figure 8.5, where it is shown that the scaling is positive for bacteria but negative for eukaryotes. The four black dots denote hypothetical species, and the red arrows denote the universal reduction in cell size and growth rate in response to reduced nutrient supplies. **B)** The joint response of cell size and growth rate to changes in nutrient availability and temperature for an arbitrary genotype. The slopes and end points of the lines are arbitrarily placed, although it is known that r_{\max} is reduced at lower temperatures (downward progression of dots), and the overall expectation is that when nutrient concentrations are manipulated so that cells are dividing at the same rates at different temperatures, cell size will be larger at the lower temperatures (rightward progression of colored lines).

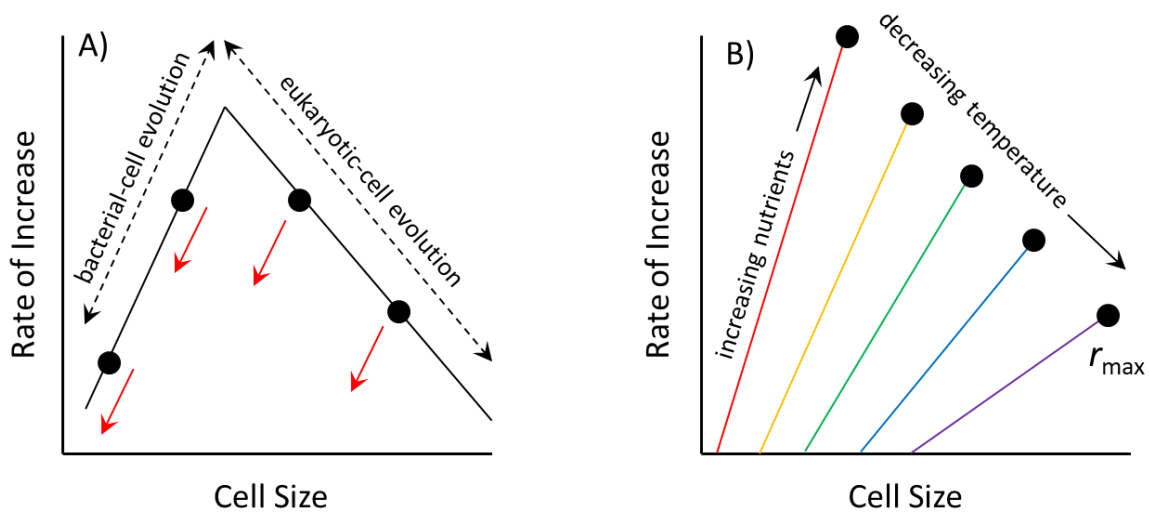


Figure 9.8. Pearson type-III distributions fitted to data on the frequency distributions of cell-division times for two species of the bacterium *Bacillus*. From Powell (1958).

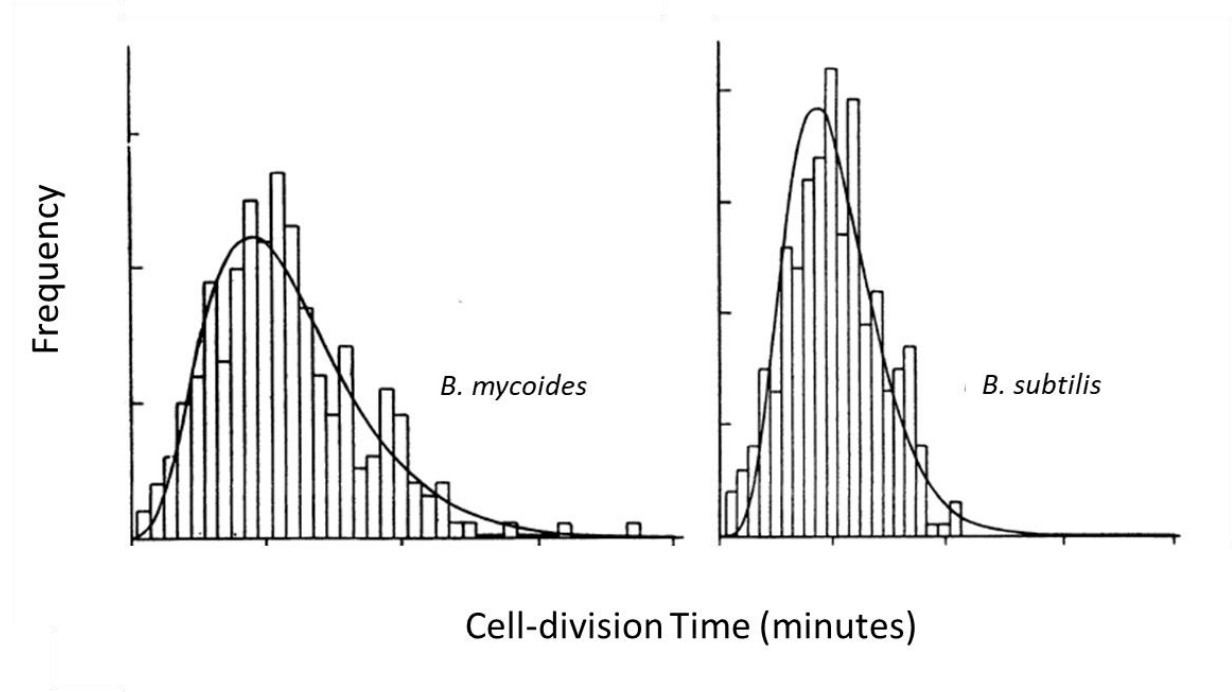


Figure 9.9. Coefficient of variation for the number of molecules inherited by daughter cells as a function of the coefficient of variation for volume of sister cells, $CV(V)$, resulting from slight asymmetries in division. Results are given for different mean numbers of molecules expected in parent cells, \bar{n} , relative to the case with simple binomial sampling, as calculated with Equation 9.9. The coefficient of variation for the number of molecules per parent cell, $CV(n_0)$, is assumed to equal 0.1 (based on empirical estimates described in the text).

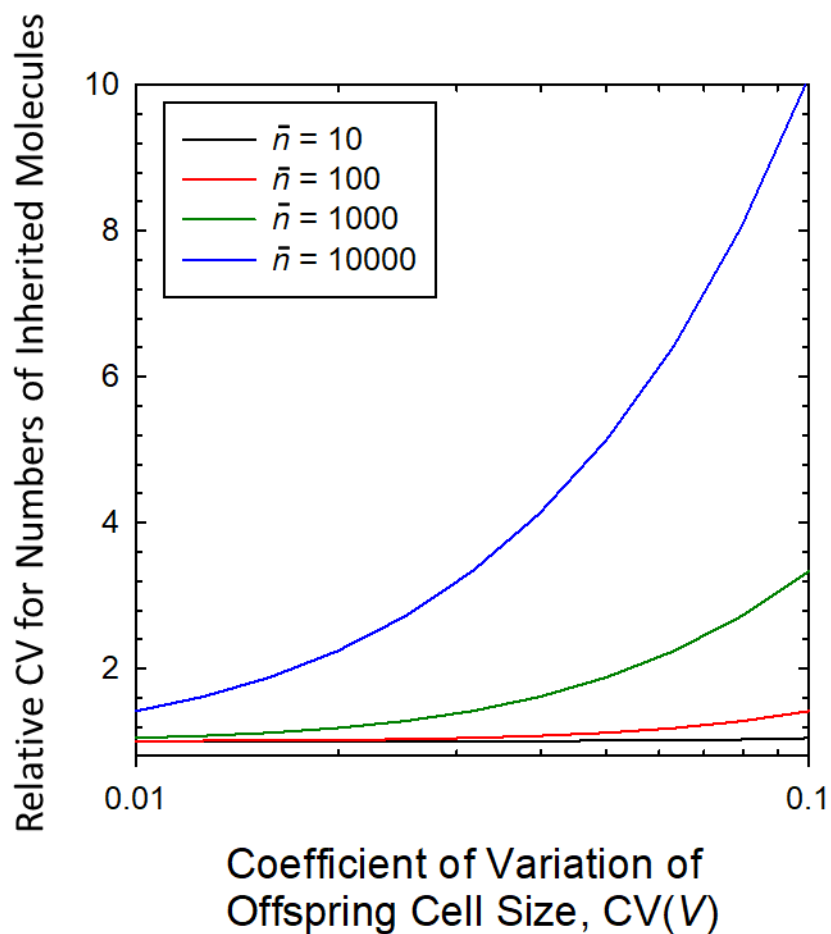


Figure 9.10. The response to directional selection for increased phenotypic values of a continuously distributed trait, represented by the transition of the black to the red bell-shaped curve. The difference between mean phenotypes after and before selection, but before reproduction, is known as the selection differential. The response to selection is determined by the degree to which offspring phenotypes resemble those of their parents, as illustrated by the diagonal dashed line. The slope of this line is known as the heritability of the trait. In the absence of genetic variation, this regression line will have a slope equal to zero. Regardless of the heritability, in the absence of selection, the offspring mean phenotype is expected to equal that of the parental generation.

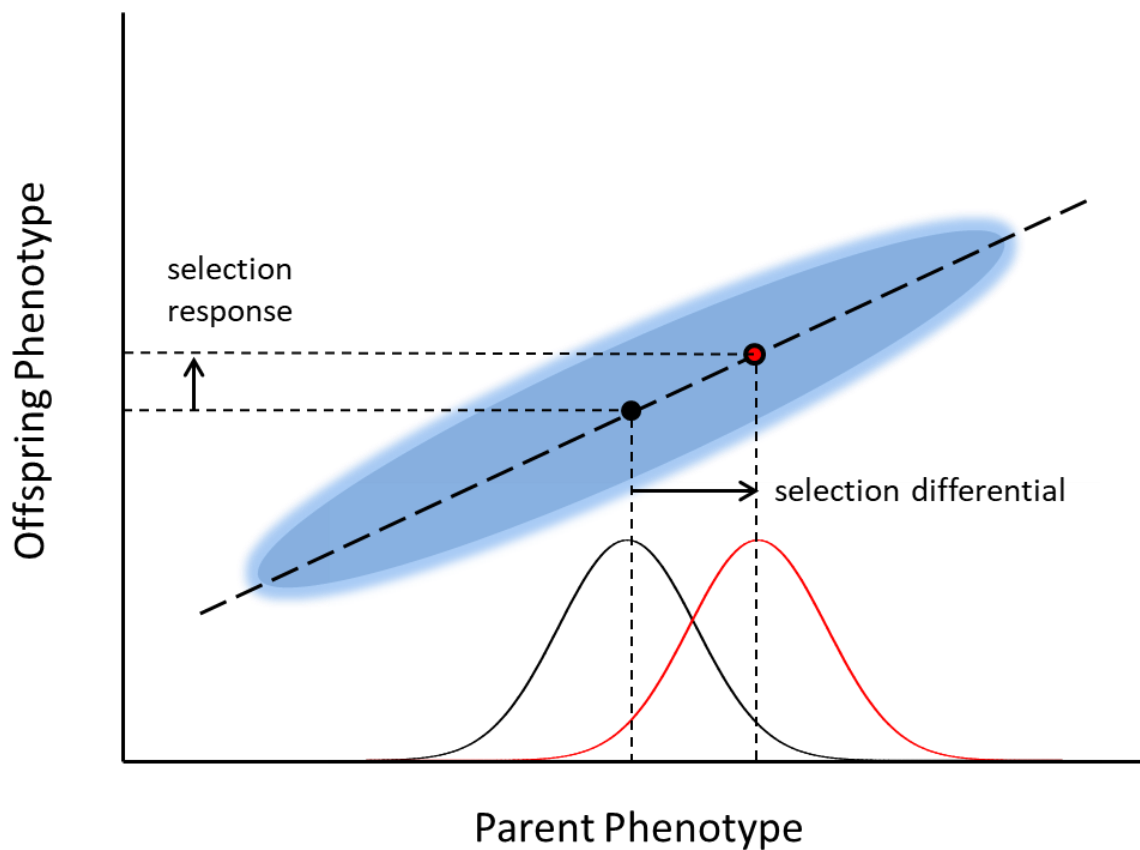


Figure 9.11. The influence of the form of the fitness function on the average fitness of a population of cells. The red lines are fitness functions denoting relationships between fitness and phenotype, and the dashed lines demarcate the expected fitnesses for three phenotypes, with the flanking two being equidistant from the one in the middle. In the absence of phenotypic variation, the mean fitness will be equal to the expectation for the middle phenotype (thick dashed lines), whereas in the presence of variation (here, assumed to be symmetrical around the mean), the average fitness for the population (blue arrows) will deviate in a direction depending on the curvature of the fitness function.

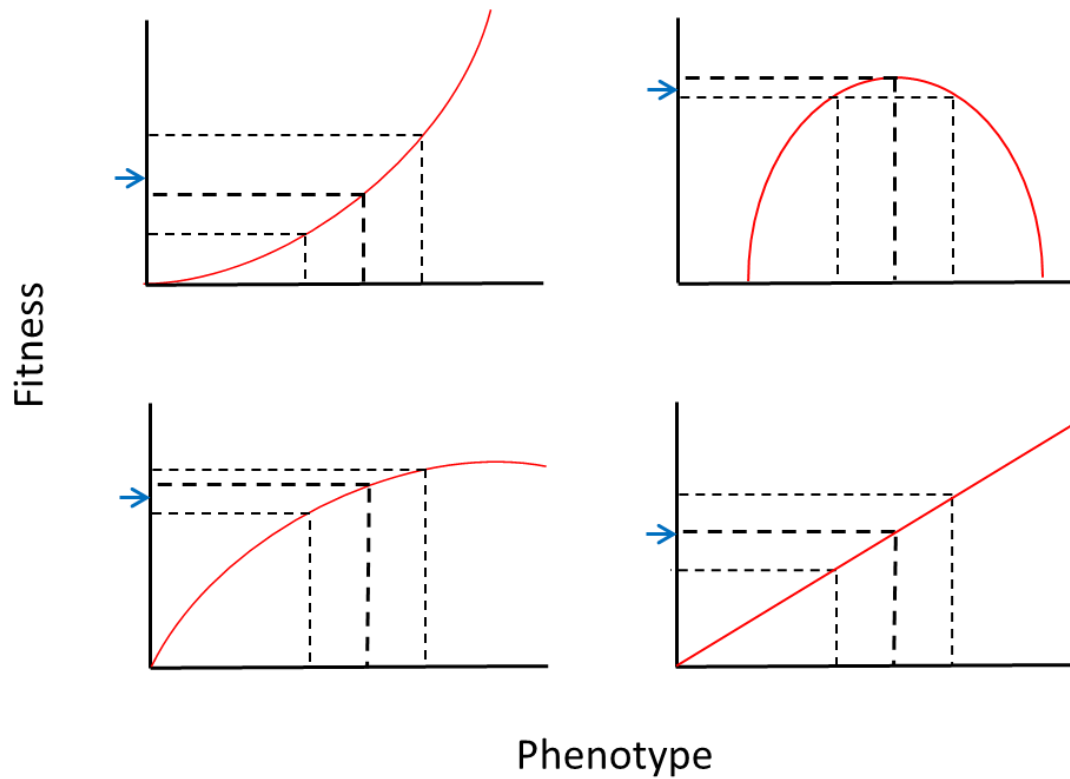


Figure 9.12. A conceptualized partitioning of total cellular proteins into three general sectors, one of which (blue) contributes an invariant proportion to the total pool regardless of the cellular nutritional state (after Scott et al. 2010). The total pool of ribosomal proteins is also considered to contain a small invariant fraction associated with inactive ribosomes (red). This leaves the pools of active ribosomal proteins (yellow) and metabolic proteins (green) free to vary with respect to each other (i.e., the green-yellow boundary associated with the double-headed arrow can move), but constrained to sum to areas under the yellow and green sectors.

